TAMPERE UNIVERSITY OF TECHNOLOGY

BIJAYA SHRESTHA

NEAR-FIELD FAR-FIELD RFID READER ANTENNA FOR EUROPEAN UHF BAND

Master of Science Thesis

Examiners: Adjunct Professor Leena Ukkonen and Professor Lauri Sydänheimo
Department of Electronics
Faculty Council Meeting: 17 August 2011

ABSTRACT

TAMPERE UNIVERSITY OF TECHNOLOGY
Master's Degree Programme in Radio Frequency Electronics
SHRESTHA, BIJAYA: Near-Field Far-Field RFID Reader Antenna for European UHF Band
Master of Science Thesis, 75 pages
August 2011
Major: Radio Frequency Electronics
Examiners: Adj. Prof. Leena Ukkonen and Prof. Lauri Sydänheimo
Keywords: Radio frequency identification technology, near field, far field, UHF, reader antenna.

Radio Frequency Identification (RFID) technology is used for identifying near or distant objects wirelessly. Near-field or far-field operations are performed to detect the tags depending on the objects and applications. UHF near-field reading is prefered for item-level tagging of small, sensitive, and expensive objects. Far-field operation is required to identify the objects farther than half a meter. Both of these reading performances may be required for inventory control of different products in supply chain management system. This thesis report presents two RFID reader antennas each working for both the near field and far field at European UHF band.

Loop is used for inductively coupled near-field performance. Segmentation of the loop and insertion of capacitors in between the segments is done to make the loop size electrically small at UHF band so as to provide uniform magnetic field over the loop surface nearby. This enables loop to detect near-field tags effectively. The first antenna implements the loop structure for near-field operation and patch structure for far-field operation. With 8 mm button type near-field tag, read range varies from 0 (at center) to 9 cm (at periphery). The far-field performance is good with realized gain of about 4 dBi and read-range of greater than 5 m with UPM short dipole tag. The antenna works from 864 to 873 MHz with $|S_{11}|$ at least 10 dB. The second antenna has only the segmented loop. The segments connected to the feed are treated as a dipole for far-field operation. The maximum near-field and far-field read range toward +z-axis with the abovementioned tags are 15 cm and 2.5 m respectively. The near-field performance is more stable than that of the first antenna.

Both of these antennas can be used in inventory control purpose requiring both the near-field and far-field operations. However, use of reflector is better for unidirectional radiation pattern in the second design and miniaturized technique of patch design can be implemented for reducing the effect of patch on near-field performance for the first design.

PREFACE

This thesis work has been carried out in Tampere University of Technology, Department of Electronics, Rauma Research Unit as a part of FIDIPRO research project applied electromagnetic systems for advanced future wireless electronics. This thesis has been supervised by adjunct professor Leena Ukkonen and professor Lauri Sydänheimo. I would like to thank Dr. Leena Ukkonen for giving me an opportunity to work on my thesis in RFID group, Department of Electronics, Tampere University of Technology. The work maintained its speed due to her continuous support, guidance, and providing good working environment from the beginning to the end. I am grateful to professor Lauri Sydänheimo for his support and making me aware of several mistakes throughout. It is a pleasure to thank FIDIPRO professor Atef Elsherbeni, from University of Mississippi, USA for his valuable comments, suggestions, and keeping track of my progress.

I am indebted to Toni Björninen for teaching me HFSS software, participating in several discussions to solve my problems, and valuable suggestions to improve my work. I should not forget Ali Babar and Juha Virtanen for their help in fabrication and measurements of my antennas.

I would like to show my gratitude to my parents for their love, support, and motivation throughout my life. Last but not the least, special regards go to all who helped me in any form to complete my work.

Tampere, August 2011

Bijaya Shrestha
bijaya_stha@hotmail.com

CONTENTS

LIST OF ABBREVIATIONS

AC	Alternating Current
CDMA	Code Division Multiple Access
DC	Direct Current
EIRP	Effective Isotropically Radiated Power
ERP	Effective Radiated Power
ETSI	European Telecommunications Standards Institute
FCC	Federal Communications Commission
FEM	Finite Element Method
FNBW	First Null Beamwidth
FR4	Flame Retardant Laminate
FSK	Frequency Shift Keying
HPBW	Half Power Beamwidth
HF	High Frequency
HFSS	High Frequency Structure Simulator
IFF	Identification Friend or Foe
ISM	Industrial, Scientific, and Medical
IEEE	Institute of Electrical and Electronics Engineers
IC	Integrated Chip
ID	Identification
LF	Low Frequency
PSK	Phase Shift Keying
QAM	Quadrature Amplitude Modulation
RFID	Radio Frequency Identification
SMA	SubMiniature version A Connector
SNR	Signal to Noise Ratio
TEM	Transverse Electromagnetic
UHF	Ultra High Frequency
VNA	Vector Network Analyzer

LIST OF SYMBOLS

ρ	Electric Charge Density (C/m^3)
ρ_s	Surface Charge Density (C/m^2)
μ	Permeability (Henry/m)
ϵ	Permittivity (Farad/m)
ϵ_r	Relative Permittivity
ϵ_{reff}	Effective Relative Permittivity
χ_e	Electric Susceptibility
χ_m	Magnetic Susceptibility
ω	Angular Frequency (rad/s)
η	Intrinsic Impedance (Ω)
σ	Electric Conductivity (S/m)
γ	Propagation Constant
$\overrightarrow{A}$	Magnetic Vector Potential (Wb/m)
$\overrightarrow{B}$	Magnetic Flux Density (Wb/m^2)
C	Coupling Coefficient
$\overrightarrow{D}$	Electric Flux Density (C/m^2)
$\overrightarrow{E}$	Electric Field Intensity (V/m)
f	Frequency (Hz)
$\overrightarrow{H}$	Magnetic Field Intensity (A/m)
h	Substrate Thickness
$\overrightarrow{J}$	Electric Current Density (A/m^2)
k	Wavenumber (1/m)
$\overrightarrow{M}$	Magnetic Current Density (V/m^2)
$\overrightarrow{P_e}$	Electric Polarization Vector (C/m^2)
$\overrightarrow{P_m}$	Magnetic Polarization Vector (Wb/m^2)
$\overrightarrow{S}$	Poynting Vector (W/m^2)
S_{11}	Reflection Coefficient of Input Port
v_p	Phase Velocity (m/s)

LIST OF FIGURES

LIST OF TABLES

1. INTRODUCTION

When you go to the university during off hours, you stamp your identitiy (id) card on a small device attached to the door and press your code and after that the door is unlucked. What an easy way to replace the key system with this advanced technology! The same id card can be used to access different rooms such as library, labs, sports hall, and so on but the permission is controlled by the administration depending on your needs. This is the auto-identification technology being widely used since many years. In this scenario, you are an object being identified by the wireless system in the university. This is one application of wireless auto-identification but it has hundreds of other applications in different fields.

There are two auto-identification technologies: Barcode technology and Radio Frequency Identification (RFID) technology. Barcode technology is gradually replaced by RFID technology due to the manufacture of less expensive and small tags. However, barcode technology is still popular in the markets for identifying cheap objects. There are some major advantages of RFID system over Barcode; RFID tag has memory to store additional information about the object, RFID can be implemented for non line of sight condition which enables the system to identify the objects far away. On the other hand, barcode technology does not have additional memory and requires line of sight which impairs the data management system and read-range performance. Though RFID was developed during the second world war, it became popular in the retail and supply chain market since 90s after the manufacture of cheap and small RFID tags.

The implementation of RFID technology in supply chain management system is increasing gradually, in which the individual objects are tracked from production level to point-of-sale. The choice of near-field or far-field system depends on several factors such as types of objects and applications. If only the small detection range is required, near-field communication is appropriate. The performance of inductively coupled near-field system is not much affected by the metal and liquid objects and the objects with high permittivity. Therefore, near-field communication is better to be used for detecting such objects. Due to larger bandwidth available as compared to LF/HF systems, UHF near-field system is becoming popular in item level tagging

of small, expensive, and sensitive objects such as gold ornaments, medical products, and pharmaceutical logistics. The reduced size of tags, and interference minimization technique are additional advantages of UHF over LF/HF systems. In supply chain management, the inventory control of products is done at several stages: in the factory warehouse, during transportation, and in the distribution warehouse to keep them in track and to update the information. So, reader units and antennas are required at different places. Near-field reader antennas read only the objects having coil tags whereas far-field reader antennas read far-field tags (esp. dipole). If we have reader antennas that read both kinds of tag, then the same antenna fulfils both the tasks. We are interested in this kind of reader antenna working in European UHF band. Designing such an antenna is really the challenging task.

Inductively coupled near-field system implements coils for both the reader and tag antennas. At LF/HF bands, the optimal size of the reader antenna is electrically small whereas it is electrically large at UHF band. In other words, the loop size is very small fraction of wavelength at LF/HF and is comparable to wavelength at UHF. For electrically small loop, the current flow is unidirectional, and its magnitude and phase are uniform along the entire loop so that the magnetic field produced is uniform on the entire region enclosed by the loop. This is required for detecting the near-field tags from the loop's surface area. For electrically large loop, the current reverses its direction at every half-wavelength and its magnitude is not uniform as well. This cannot provide the uniform field distribution over the loop surface due to the superposition of fields produced by non-uniform current segments. The current distribution can be made uniform by segmenting the loop and inserting capacitors in between each pair of segments. This technique is used to design the near-field reader antenna at UHF band. The additional structure can be implemented to add the feature of far-field reader-antenna. This thesis report presents two antennas working for both near-field and far-field. The first antenna implements segmented loop for near-field and patch structure for far-field, whereas the second antenna implements only the segmented loop to achieve both the performances. The feed-connected segments forming a dipole like structre are used for far-field radiation.

The whole report is divided into eight segments. The first chapter is "Introduction" itself. The basic laws and phenomena about electromagnetism are presented in the second chapter "Electromagnetic Basics". This is important to know before entering to the world of antenna. Since we are making antennas for RFID applications, basic knowledge about RFID technology and its terminology is required which is described in the third chapter "Basics of RFID". There are different designs for RFID reader antennas whose help was needed to start the design process of our

antennas. This is discussed in the fourth chapter “RFID Reader Antennas”. The fifth chapter “Segmented Loop Antenna With Patch” is the experimental part for the first antenna. Design process, simulations, fabrication, and measurements of segmented loop with patch reader antenna are well described in this chapter. From design to measurements of the second reader antenna with only the segmented loop is described in the sixth chapter “Segmented Loop Antenna”. Both of these antennas are near-field far-field reader antennas at UHF band. Therefore, it is good to compare their performances which is done at the seventh chapter “Comparisons”. Finally, the whole thesis work is summarized in the last chapter “Conclusion”.

2. ELECTROMAGNETIC BASICS

Knowledge of electromagnetics is inevitable in antenna design related works because it involves electromagnetic phenomena such as electromagnetic wave proagation, electric field and magnetic field coupling and so on. The electromagnetic phenomena can be well studied with the help Maxwell's equations which will be discussed in the following section. This chapter will review some important topics in electromagnetics.

2.1 Maxwell's Equations

Maxwell's equations tell us about the electric and magnetic phenomena. These equations are based on the works done by Gauss, Ampere, and Faraday. The time-varying Maxwell's equations in point (or differential) form are [1]

$$\nabla \times \overrightarrow{E} = \frac{-\partial \overrightarrow{B}}{\partial t} - \overrightarrow{M}, \tag{2.1}$$

$$\nabla \times \overrightarrow{H} = \frac{\partial \overrightarrow{D}}{\partial t} + \overrightarrow{J}, \tag{2.2}$$

$$\nabla \cdot \overrightarrow{D} = \rho, \tag{2.3}$$

$$\nabla \cdot \overrightarrow{B} = 0. \tag{2.4}$$

Where $\overrightarrow{E}$ is the electric field intensity (V/m), $\overrightarrow{H}$ is the magnetic field intensity (A/m), $\overrightarrow{D}$ is the electric flux density (C/m^2), $\overrightarrow{B}$ is the magnetic flux density (Wb/m^2), $\overrightarrow{M}$ is the (fictious) magnetic current density (V/m^2), $\overrightarrow{J}$ is the electric current density (A/m^2), and ρ is the electric charge density (C/m^3).

The constitutive properties of the medium are expressed as

$$\overrightarrow{B} = \mu \overrightarrow{H}, \tag{2.5}$$

$$\overrightarrow{D} = \epsilon \overrightarrow{E}, \tag{2.6}$$

where, μ, and ϵ are the permeability and permittivity of the medium. For the free space, $\mu = \mu_0 = 4\pi \times 10^{-7}$ (Henry/m), and $\epsilon = \epsilon_0 = 8.854 \times 10^{-12}$ (Farad/m).

2.2 Fields in Media

When the fields are applied in different media than free space, there is complexity in the analysis. Let us consider the medium to be dielectric. The polarization [1] occurs when an electric field $\overrightarrow{E}$ is applied to this dielectric material and the total displacement flux becomes

$$\overrightarrow{D} = \epsilon_0 \overrightarrow{E} + \overrightarrow{P}_{\mathrm{e}}, \tag{2.7}$$

where, $\overrightarrow{P_e}$ is the polarization vector given by

$$\overrightarrow{P_e} = \epsilon_0 \chi_{\mathrm{e}} \overrightarrow{E}. \tag{2.8}$$

Here, χ_e is the electric susceptibility. Now,

$$\overrightarrow{D} = \epsilon_0 \overrightarrow{E} + \overrightarrow{P}_{\mathrm{e}} = \epsilon_0 (1 + \chi_{\mathrm{e}}) \overrightarrow{E} = \epsilon \overrightarrow{E}, \tag{2.9}$$

$$\text{where } \epsilon = \epsilon' - j\epsilon''. \tag{2.10}$$

This is the complex permittivity of the medium. The imaginary part of ϵ accounts for the loss.

Let us consider a medium to be magnetic material. Magnetic polarization [1] occurs by the application of magnetic field resulting the magnetic flux density to be

$$\overrightarrow{B} = \mu_0 (\overrightarrow{H} + \overrightarrow{P_{\mathrm{m}}}), \tag{2.11}$$

where $\overrightarrow{P_m} = \chi_{\mathrm{m}} \overrightarrow{H}$ is the magnetic polarization vector and χ_m is the magnetic susceptibility. Now,

$$\overrightarrow{B} = \mu_0 (1 + \chi_{\mathrm{m}}) \overrightarrow{H} = \mu \overrightarrow{H}, \tag{2.12}$$

where $\mu = \mu_0(1 + \chi_m) = \mu' - j\mu''$ is the complex permeability of the medium. The imaginary part here also causes loss in the medium.

2.3 Boundary Conditions

The boundary conditions give us the idea about the electromagnetic behaviour at the interface between two different media. Electric field and magnetic field must fulfil the boundary conditions at the interface. The subscript “t”, and “n” denote for tangential and normal components respectively.

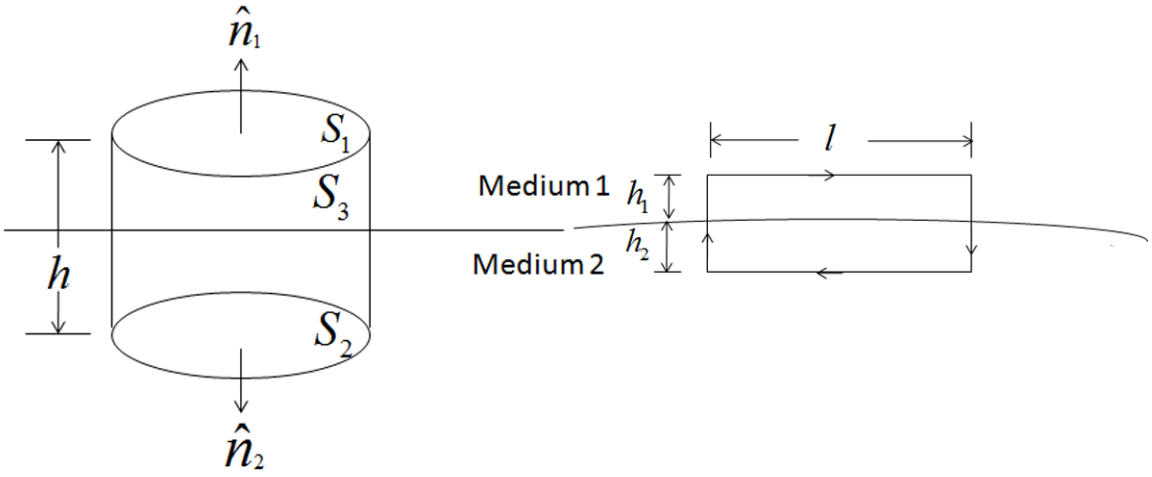

Figure 2.1: Boundary Conditions for Normal (Left) and Tangential (Right) Field Components [2].

Starting with one of the Maxwell's equations, $\nabla \cdot \overrightarrow{B} = 0$, the divergence theorem can be applied over the volume enclosed by the surfaces S_1, S_2, and S_3, so as to get

$$\oint_S \overrightarrow{B} \cdot \hat{n}\ ds = \int_{S_1} \overrightarrow{B} \cdot \hat{n}_1\ ds + \int_{S_2} \overrightarrow{B} \cdot \hat{n}_2\ ds + \int_{S_3} \overrightarrow{B} \cdot \hat{n}_3\ ds = 0. \tag{2.13}$$

If h approaches zero, then the last term ceases and the above expression can be directly stated as

$$B_{1n} = B_{2n}. \tag{2.14}$$

Considering another Maxwell's equation: $\nabla \times \overrightarrow{E} + \frac{\partial \overrightarrow{B}}{\partial t} = 0$, we can integrate it over the surface bounded by a rectangular loop as shown in the right part of the Figure 2.1.

$$\int_S \nabla \times \overrightarrow{E} \cdot \hat{n}\ ds = -\int_S \frac{\partial \overrightarrow{B}}{\partial t} \cdot \hat{n}\ ds. \tag{2.15}$$

Application of Stoke's theorem results

$$\oint_C \overrightarrow{E} \cdot \overrightarrow{l} = -\int_S \frac{\partial \overrightarrow{B}}{\partial t} \cdot \hat{n}\ ds, \tag{2.16}$$

$$\text{Or, } lE_{1t} - lE_{2t} + h_1E_{1n} + h_2E_{2n} - h_1E'_{1n} - h_2E'_{2n} = -\int_S \frac{\partial \overrightarrow{B}}{\partial t} \cdot \hat{n}\ da. \tag{2.17}$$

Letting h_1 and h_2 approach zero, the last four terms on the left side become zero. At the same time, the right hand side term also vanishes because of no surface area.

This leaves us the simple expression as given by

$$E_{1t} = E_{2t}. \tag{2.18}$$

This expression states that the tangential component of $\overrightarrow{E}$ is continuous across the interface.

Let us determine the boundary condition of normal component of the electric flux density. Maxwell equation: $\nabla \cdot \overrightarrow{D} = \rho$ and left part of the Figure are implemented for this purpose. Volume integration of this expression gives

$$\int_V \nabla \cdot \overrightarrow{D}\ dv = \int_v \rho\ dv. \tag{2.19}$$

Divergence theorem is applied so that the above expression can be written as

$$\oint_S \overrightarrow{D} \cdot \hat{n}\ d\overrightarrow{s} = \int_v \rho\ dv. \tag{2.20}$$

For $h \to 0$, the tangential part becomes zero and the above expression is simplified to

$$D_{1n} - D_{2n} = \rho_s, \tag{2.21}$$

where ρ_s is the surface charge density on the interface.

Final boundary condition is for the tangential component of the magnetic field intensity. Integrating the Maxwell equation: $\nabla \times \overrightarrow{H} = \frac{\partial \overrightarrow{D}}{\partial t} + \overrightarrow{J}$ over the surface area enclosed by a rectangular loop as shown in the right part of the Figure and applying the same steps as done for electric field intensity, we get

$$H_{1t} - H_{2t} = J_s, \tag{2.22}$$

where J_s is the surface current density that exists on the interface.

2.4 Plane Waves

Let us consider a source-free medium which is linear, isotropic, and homogeneous. The Mawell's equations (2.1), and (2.2) in phasor form for this medium are [1]

$$\nabla \times \overrightarrow{E} = -j\omega\mu\overrightarrow{H}, \text{and} \tag{2.23}$$

$$\nabla \times \overrightarrow{H} = -j\omega\epsilon\overrightarrow{E}, \tag{2.24}$$

where ω is the angular frequency. Applying curl to (2.23) and using (2.24) gives [1]

$$\nabla \times \nabla \times \overrightarrow{E} = -j\omega\mu\nabla \times \overrightarrow{H} = \omega^2\mu\epsilon\overrightarrow{E}. \tag{2.25}$$

We have vector identity: $\nabla \times \nabla \times \overrightarrow{A} = \nabla(\nabla \cdot \overrightarrow{A}) - \nabla^2\overrightarrow{A}$. This identity leads (2.25) to

$$\nabla^2\overrightarrow{E} + \omega^2\mu\epsilon\overrightarrow{E} = 0. \tag{2.26}$$

This is the wave equation for $\overrightarrow{E}$. The wave equation for $\overrightarrow{H}$ can be derived similarly to be

$$\nabla^2\overrightarrow{H} + \omega^2\mu\epsilon\overrightarrow{H} = 0. \tag{2.27}$$

2.4.1 Lossless Medium

For solving the plane wave equations, we consider only one field component; x-component of $\overrightarrow{E}$. There is no variation of this field in x- and y-directions except in z. Thus, (2.26) can be written as [1]

$$\frac{\partial^2 E_x}{\partial z^2} + k^2 E_x = 0., \tag{2.28}$$

where $k = \omega\sqrt{\mu\epsilon}$ is the wavenumber (1/m), or propagation constant of the medium. For lossless medium, μ and ϵ are real numbers. The solutions to (2.28) are given as

$$E_x(z) = E^+e^{-jkz} + E^-e^{jkz}. \tag{2.29}$$

In the time domain,

$$E_x(z,t) = E^+\cos(\omega t - kz) + E^-cos(\omega t + kz). \tag{2.30}$$

The first term is the wave travelling in the +z direction and the second term in the -z direction. The phase velocity is given by

$$v_p = \frac{1}{\sqrt{\mu\epsilon}}. \tag{2.31}$$

The magnetic field wave can be obtained by substituting (2.29) in (2.23).

$$H_y = \frac{1}{\eta}[E^+e^{-jkz} - E^-e^{jkz}], \tag{2.32}$$

where $\eta = \sqrt{\mu/\epsilon}$ is the wave impedance for the plane wave. The electric field and the magnetic field are orthogonal to each other and are propagating to the direction which is orthogonal to both of them. Such electromagnetic wave is known as the

transverse electromagnetic (TEM) wave.

2.4.2 Lossy Medium

For a conducting medium with conductivity σ, the wave equation for $\overrightarrow{E}$ can be derived as [1]

$$\nabla^2 \overrightarrow{E} + \omega^2 \mu\epsilon \left(1 - j\frac{\sigma}{\omega\epsilon}\right) \overrightarrow{E} = 0. \tag{2.33}$$

The propagation constant is defined here as

$$\gamma = \alpha + j\beta = j\omega\sqrt{\mu\epsilon}\sqrt{1 - j\frac{\sigma}{\omega\epsilon}} \tag{2.34}$$

The wave equation for the electric field with only the x-component propagating in z-axis becomes

$$\frac{\partial^2 E_x}{\partial z^2} - \gamma^2 E_x = 0. \tag{2.35}$$

The solutions to (2.35) are

$$E_x(z) = E^+ e^{-\gamma z} + E^- e^{\gamma z} \tag{2.36}$$

Here, $e^{-\gamma z} = e^{-\alpha z} e^{-j\beta z}$. This gives the wave traveling in the $+z$ direction with exponential decay by $e^{-\alpha z}$. The magnetic field can be deduced as

$$H_y(z) = \frac{-j\gamma}{\omega\mu} \left(E^+ e^- \gamma z - E^- e^{\gamma z}\right). \tag{2.37}$$

The wave impedance for lossy medium is

$$\eta = \frac{j\omega\mu}{\gamma}. \tag{2.38}$$

2.5 Poynting Theorem

Poynting theorem [3] is expressed as

$$-\oint_S (\overrightarrow{E} \times \overrightarrow{H}) \cdot d\overrightarrow{s} = \int_V \overrightarrow{J} \cdot \overrightarrow{E}\, dv + \frac{d}{dt}\int_V \frac{1}{2}\overrightarrow{D} \cdot \overrightarrow{E}\, dv + \frac{d}{dt}\int_V \frac{1}{2}\overrightarrow{B} \cdot \overrightarrow{H} dv. \tag{2.39}$$

The first integral on the right side is the total ohmic power dissipated within the volume. The second and the third integral are the total energy stored in the electric field and the magnetic field respectively. The last two integrals give the time rates of increase of energy stored within the volume, or the instantaneous power going to increase the stored energy. Thus, the sum of the expressions on the right side is the

total power flowing into the volume, and the total power leaving the volume is

$$\oint_S (\overrightarrow{E} \times \overrightarrow{H}) \cdot d\overrightarrow{s} (\mathrm{W}), \tag{2.40}$$

where the cross product between $\overrightarrow{E}$ and $\overrightarrow{H}$ is regarded as the Poynting vector, $\overrightarrow{S}$. i.e.,

$$\overrightarrow{S} = \overrightarrow{E} \times \overrightarrow{H} (\mathrm{W/m^2}). \tag{2.41}$$

Poynting vector is referred to as an instantaneous power density whose direction is the direction of the instantaneous power flow at a point.

3. BASICS OF RFID

Radio Frequency Identification (RFID) is the technology of identifying an object at distance wirelessly. It has many advantages over conventional bar-code technology. Unlike bar-code, RFID technology works for longer distance and does not require line of sight. RFID tags can store additional information such as manufacturer, product type, and others [4], [5]. Though RFID has existed for more than half a century, its popularity increased after the manufacture of inexpensive ICs for low-cost RFID tags. In addition to low cost, the tags must be compact, mechanically robust, and readable from couple of meters away. RFID has been applied in the manufacture and distribution of goods since mid 90s. It was adopted by the United States for the rail industry and by Singapore for traffic management during that time. The tracking of human beings and animals was also begun with the implementation of RFID in 90s [4], [6].

While going back to its history, RFID technology was used by Britain in the second world war for the first time to identify the aircrafts using the IFF (Identification Friend or Foe) system. The initial phase used only a single bit of information. The United States and Britain improved the technology from a single bit to several bits of ID space so that many aircrafts could be recognized with their own unique IDs and information exchange would be possible. The cost of transponders (RFID tags) is not barrier for this application because the aircrafts are very much expensive as compared to them. But, for smaller and less-expensive objects than airplanes, the cost, size, and the complexity should be reduced. In the 1960s, Los Alamos National Laboratory implemented RFID to automatically identify people for limiting the access to secure areas. RFID has been used also to identify animals, label airline luggage, make toys interactive, prevent theft, and locate lost items [4]. The more information about basics of RFID and applications can be found in [4], [5], [6], [7], and [8].

3.1 Frequency Ranges and Power Regulations

Every wireless technology is assigned certain frequency band at different center frequencies to avoid interference among different radio systems. The frequency allocations may be different for different countries. Certain frequency bands are allocated

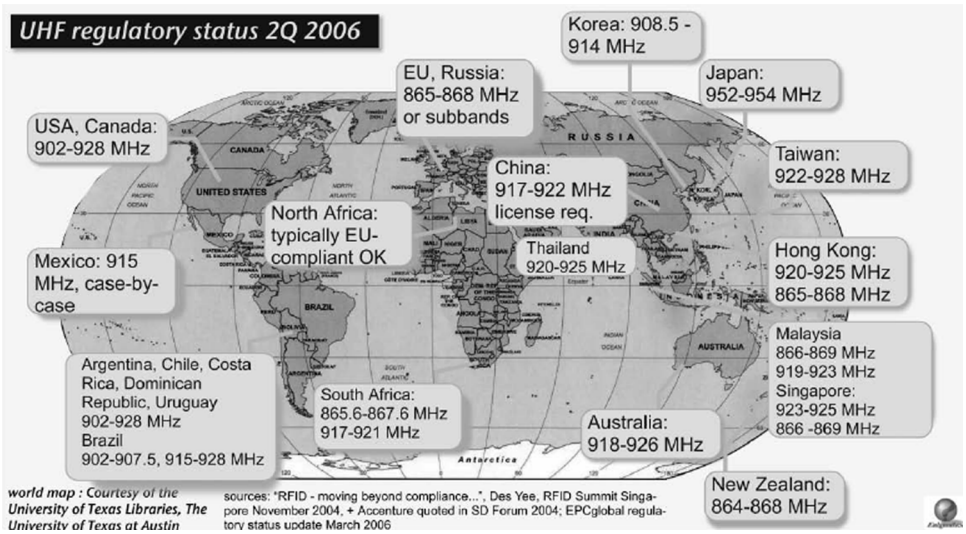

Figure 3.1: UHF Bands for RFID in Different Countries [6].

for industrial, scientific, and medical applications which are known as ISM bands. RFID uses the ISM bands in addition to the frequency range below 135 kHz [7].

RFID is operated at several bands: low frequency (LF), high frequency (HF), ultra high frequency (UHF), and microwave frequency. The most common frequency bands are LF: $<$ 135 kHz, HF: 13.56 MHz, UHF: 860 - 960 MHz, and 2.4 - 2.45 GHz [6]. Though the frequency band 2.4 - 2.45 GHz lies in the UHF band, it is generally referred to as the microwave band. UHF band is widely used for RFID applications due to its major advantages like high speed data rate and simple antenna structures as compared to the other bands. Different countries have allocated different frequency bands in UHF as seen clearly from the Figure 3.1.

Power regulation is also an important act to avoid interferences produced by nearby transmitters operating in the same frequency band. The maximum transmitted power is limited that varies from region to region. There are different regulatory bodies for frequency band allocations and power transmission limitations. Federal Communications Commission (FCC) is the one that licenses the spectrum and regulates the power transmission in the United States of America (USA). The part 15 of FCC documents deals with the regulations of unlicensed spectrum. For the frequency range: 902 - 928 MHz, the maximum transmitted power is limited to 1 W. The maximum effective isotropically radiated power (EIRP) is 4 W or 36 dBm. Therefore, transmitted power should be reduced if the antenna gain is greater than 6 dBi [9], [10]. The relationship between EIRP and effective readiated power (ERP) is given by EIRP $= 1.64 \times$ ERP. This implies that the corresponding ERP is 2.4 W.

European Telecommunications Standards Institute (ETSI) is the similar regulatory body for Europe. The document *ETSI 302 208* says that the allowed UHF band for RFID in Europe is 865 - 868 MHz and the maximum ERP is 2 W [10], [11].

3.2 LF/HF vs. UHF RFID

Inductive coupling is used in LF/HF bands where antenna size is smaller than the wavelength. The magnetic field strength decays rapidly as $1/r^3$ when tag moves away from the reader antenna. Therefore, the read-range is small which is comparable to the size of the reader antenna. This system implements coils as the antennas. LF/HF RFID is used for those objects which have in their vicinity liquids and other objects with high permittivity because this system is unaffected by their presence [6].

UHF RFID implements electromagnetic coupling in which antenna size is comparable to the wavelength. It has higher read-range because the power falls slowly as the square of distance between the reader antenna and the tag. It is more prone to interference due to the complex propagation environment. Dipole antennas are normally used in this system. Data rate is higher because it has larger bandwidth than LF and HF systems. It has been used in rail-car tracking, automobile tolling, supply chain management, and other various applications where the read-range should be from couple of meters to several meters [6].

3.3 Classification of Tags

The RFID tags are classified into the three following categories [6] according to the use of power supply method.

1. **Passive Tags:** have no source of power by their own. They receive the transmitted wave from the reader antenna and convert it to the DC level by rectification process. A diode and a high valued capacitor are used for this conversion from ac to dc. This power is used by the circuitry in the tag. Tag uses the envelope detection method to detect the information provided by the reader. The tag changes its input impedance according to its ID which varies the reflected wave from the tag to the reader. This backscattered signal is the information sent by the tag to the reader.

2. **Semi-Passive Tags:** are also referred to as battery-assisted tags. They have their own battery integrated which is used to power the tag circuitry. The battery assists for signal amplification so that it has hundreds of meters read-range. However, the way of communications is similar to that with passive tags.

3. **Active Tags:** have both battery and transmitter unlike passive and semi-passive tags. So, active tags do not need to backscatter the signal. Instead, they can transmit signal in different frequency band. This is the bidirectional communication. The system with active tags can adopt different modulation and demodulation techniques such as phase shift keying (PSK), frequency shift keying (FSK), and quadrature amplitude modulation (QAM). This can implement also the CDMA technology. This system is therefore immune to noise and interference. The read-range can go up to few kilometers.

The active tags are not used in disposable consumer products due to the cost and complexity of integrating the battery onto the tag [12]. Therefore, passive RFID systems are normally used.

3.4 RFID System

An RFID system comprises of RFID reader (which is also known as interrogator), RFID tag (also known as transponder) and antennas. Reader antennas may be integrated with the readers or connected via cables whereas tag antennas are generally integrated with the tags. Every tag ic is assigned a tag ID which is after all the identification code for an object with the corresponding tag. The reader unit comprises of separate transmitter and receiver whereas the tag may contain only the receiver (in passive and semi-passive tags) or both (in active tags). Readers can have monostatic or bistatic configurations: monostatic if they use a single antenna for both the transmission and reception and bistatic if they use separate antennas.

The information exchange between reader and tag is through the radio link. The link associated with the data flow from reader to tag is referred to as the downlink or forward link and the reverse case is referred to as the uplink or forward link. Link budget is an important tool to determine the read-range of RFID system. It is the power required to deliver the data wirelessly from the transmitter to the receiver. The link budget depends on several factors such as transmit power, path loss, tag sensitivity, reader sensitivity, and antenna designs.

3.4.1 Near-Field Operation

Though the near-field communication can be achieved through both the electrical and magnetic coupling, the later is preferred due to its better performance in the presence of metal and liquid objects nearby [13]. Coils are used as the antennas for both the reader and the tag. The reader coil carries alternating current thereby providing alternating magnetic field in its vicinity. When the tag coil is placed in the

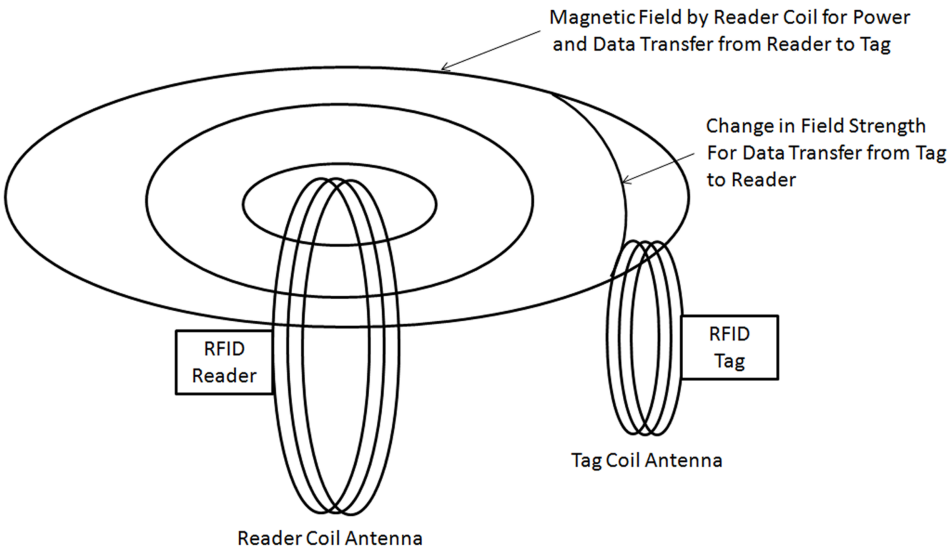

Figure 3.2: Near-Field Communication [4].

magnetic field region, the alternating voltage is induced across it. For passive tags, this ac voltage is converted into dc for circuitry operation. The communication from tag to reader is done through load modulation [4]. The small ac current induced in the tag coil produces small magnetic field which affects the magnetic field of the reader thereby changing the current flow through it. The amount of change depends on the amount of current flow through the tag which again depends on its load thus termed as the load modulation. The load of the tag coil can be changed according to the tag's ID. This variation of the load causes the variation in the current flow through the reader thereby detecting the signal sent by tag.

There are some limitations with near-field RFID system. The read-range is approximated as $c/2\pi f$ which directly specifies that it becomes smaller when operated at higher frequency. The magnetic field decays by a factor of $1/r^3$, where r is the distance between the tag and reader. Another major disadantage is the data rate; which implies the requirement of higher ID bits to read collocated tags successfully. The near-field RFID system at LF/HF has small bandwidth.

3.4.2 Far-Field Operation

The information exchange between reader and tag is carried out through the electromagnetic coupling in far-field communication system. Generally, dipole antennas are used in tags so that they can be read from all around except along the axis of the antenna. The electric potential is induced across the diode after receiving electromagnetic wave sent by the transmitter. This potential is rectified to supply the

power for tag's circuitry operation in passive RFID. The information is sent back to the reader by using *back scattering* technology [4].

When incoming signal is impedance matched to the tag antenna, all the power encountered to the antenna is absorbed. In the case of impedance mismatch, some of the power gets reflected back depending on the degree of mismatch. The antenna's impedance can be changed according to the tag's ID thereby changing the amount of reflected power. This variation in power is the back scattered signal which is detected by the reader.

4. RFID READER ANTENNAS

4.1 Antenna Field Regions

Reader antennas basically provide two types of regions: far-field and near-field [14]. In the far-field region, energy transfer is through the electromagnetic wave. The electric field and the magnetic field are related by the free-space wave impedance and decays by $1/r$, where r is the distance of a point from the center of the antenna.

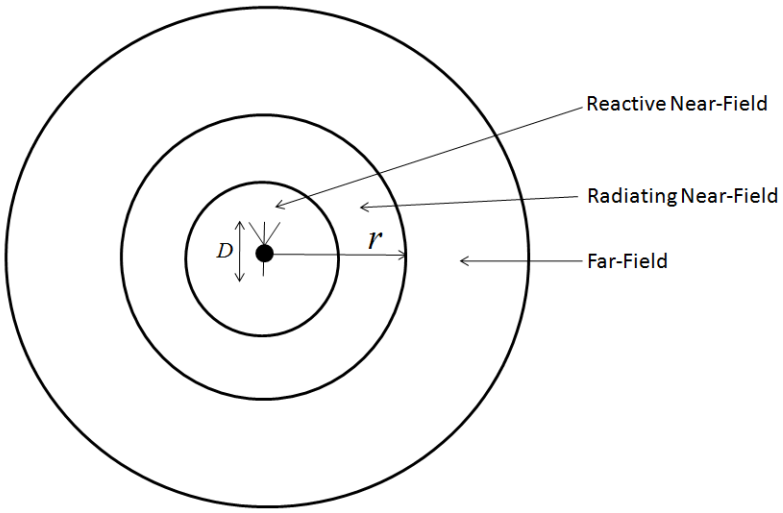

Figure 4.1: Antenna Field Regions [14].

Near-field zone can be subdivided into reactive near-field region and radiating near-field region. In the reactive near-field region, the energy is stored in the forms of electric and magnetic fields and not radiated. The ratio of electric and magnetic fields here is not equal to the free-space wave impedance. The boundary between far-field and near-field region for the electrically large antennas is given as $r = 2D^2/\lambda$, where D is the maximum antenna dimension and λ is the wavelength. Boundary of the radiating near-field region in this case is $r = 0.62\sqrt{D^3/\lambda}$ [15]. In this region, the energy is radiated as well as exchanged with the source. The radiating near-field region is negligibly small in case of electrically small antennas; and the far-field boundary is given by $r = \lambda/2\pi$.

4.2 Near-Field Operations

These antennas work in the reactive near-field region either by electical coupling or by magnetic coupling. The type of coupling is based on the antenna design. If dipole antennas are used, then energy transfer between reader and tag is through electrical coupling. Whereas, loop antennas are used for magnetic coupling. For the best data transfer, both the reader antenna and the tag antenna should be of same kind. Inductive coupling is preferred for near-field communication because it is not affected by the surrounding objects: metal,liquids, and other objects with high relative permittivity [14], [16], [17], [18], [19], [20], [21]. For inductive coupling, both the reader and the tag antennas are the coils and their coupling coefficient can be expressed as [14]

$$C \propto f^2 N^2 S^2 B^2 \alpha \tag{4.1}$$

where f is the operating frequency, N is the number of turns in tag antenna coil, S is the cross-sectional area of the coil, B is the magnetic field density at the tag location created by the reader antenna, and α is the coil misalignment loss.

The near-field RFID systems can work for low frequency (LF), high frequency (HF), and ultra high frequency (UHF). There are some advantages of using UHF over LF/HF. The near-field UHF RFID system demands smaller size tags, doesn't suffer from interference easily for close separation of tags, and has higher data rate. These advantages have led for the intense research on near-field UHF systems. Moreover, the near-field UHF RFID systems have promising performance for item-level tracking of pharmaceutical logistics, transports, medical products, and others [14], [22], [23], [24].

The performance of the near-field reader antenna is based on its read-range. The magnetic field distribution should be uniform over its interrogation zone for wide detection coverage. For LF/HF systems, loop is electrically small for significant interrogation area and hence the current distribution is almost constant with no phase variation giving the uniform magnetic field along the axis perpendicular to the loop plane. For UHF systems, the loop size should be electrically large (i.e., comparable to wavelength) to provide physically large interrogation zone. In this case, the current is not distributed uniformly. Rather, it reverses its direction for every half wavelength. As a result of which, the magnetic field along the central axis is very weak as compared to the regions near by loop.

4.2.1 Magnetic Field and Current Distribution for Different Loop Sizes

We are interested here for UHF band in European system. Simulations are done for loops with different electrical length at 866.5 MHz.

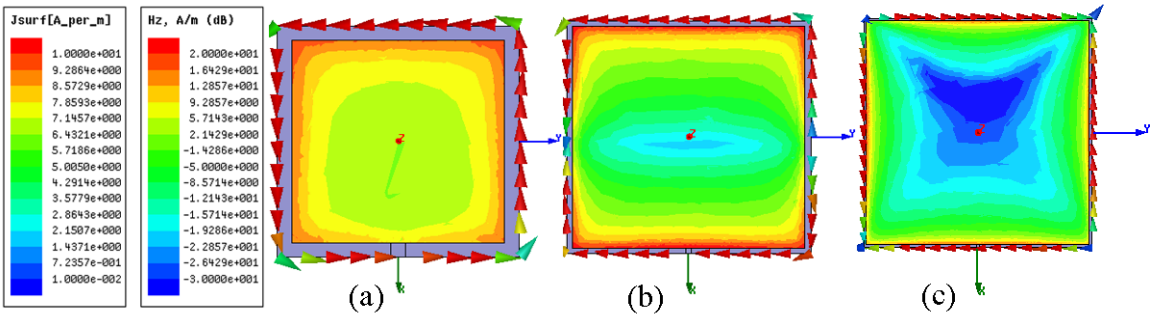

Figure 4.2: Current and z-Component Magnetic Field Distribution in Conventional Loop for Loop Perimeter of (a) $\lambda/2$, (b) λ, and (c) 2λ.

From the Figure 4.2, it is seen that the magnetic field becomes more non-uniform when the loop size is increased. It is because the current reverses its direction after every half wavelength and the current flow is non unidirectional. As a result of which, the magnetic field in the center region is cancelled out due to opposite direction of magnetic field from different sections of the loop. For the first case, the current flow is in the same direction and the magnetic field distribution is pretty much uniform. For the second case, the current is flowing in two directions and hence the field distribution is non uniform in the center region. When the loop is even increased to about 2λ as in the third case, the current changes its direction after every half-wavelength and the magnetic field gets distributed accordingly. It is now highly non-uniform.

4.2.2 UHF RFID Near-Field Antenna Design Technique

In UHF band, the loop perimeter should be comparable to the operating wavelength for optimal interrogation zone. The current distribution along the loop is no more unidirectional and the phase variations occur a lot. This cannot distribute the magnetic field uniformly on the interrogation zone. The magnetic field becomes very weak in the center region due to the superposition of fields generated by counter-phase currents [25].

This problem can be solved by dividing the antenna into short segments and introducing the capacitors in between the segments to make the loop electrically small [26]. The capacitor values are chosen such that the inductive effect of the

loop is nullified so that it is resonating at the desired frequency. In few words, the imaginary part of the antenna at the operating frequency is zero. In this condition, the current distribution is almost uniform with very little phase variations so that the magnetic field distribution is uniform.

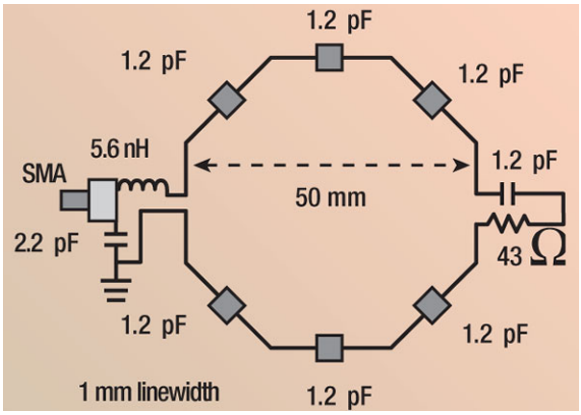

Figure 4.3: Segmented Loop [26].

4.2.3 UHF RFID Near-Field Antenna Design Reviews

There are several designs published for UHF RFID Near-field antennas. Few designs will be reviewed briefly here.

The dimensions used are $L_1 = 170$ mm, $L_2 = 28.5$ mm, $W_1 = 170$ mm, $W_2 = 2$ mm, $W_3 = 4$ mm, $R_1 = 80$ mm, and $R_2 = 45$ mm. -10 dB bandwidth is from 840 MHz to 1300 MHz. The substrate used is FR4 with thickness of 0.8 mm and relative permittivity of 4.4. The loop is segmented and the coupling between the segments provides needed capacitance. It claims that the maximum read-range for this design is 20 cm.

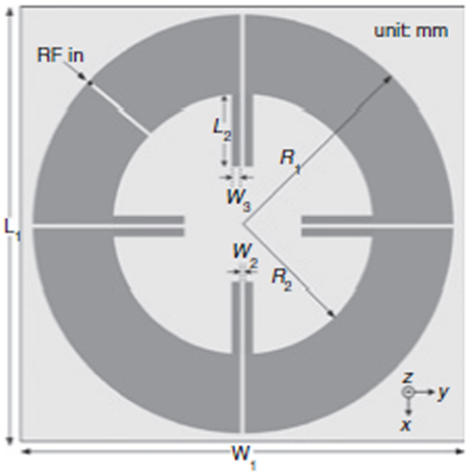

Figure 4.4: Segmented Loop Antenna Review 1 [27].

The dimensions are $L_1 = 60$ mm, $S_1 = 10$ mm, $L_2 = 58$ mm, $S_2 = 12$ mm, $L_3 = 24$ mm, $S = 0.5$ mm, and $W = 2$ mm. The substrate used is FR4 with thickness of 0.5 mm and relative permittivity of 4.4. -10 dB bandwidth is from 800 MHz to 1040 MHz. Top to bottom coupling approach is implemented here. It claims that maximum read range is 10 cm.

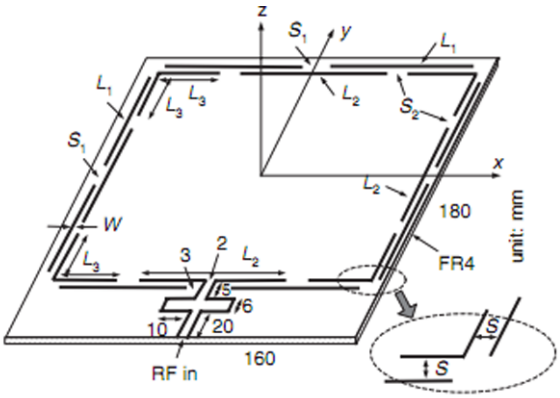

Figure 4.5: Segmented Loop Antenna Review 2 [28].

Another publication from the same authors as mentioned in the second review is also available as [24]. The above design involves top to bottom coupling, whereas the following is side by side coupled design. It uses the similar substrate: FR4 with $\epsilon_r = 4.4$, $\tan\delta = 0.02$, and thickness $h = 0.5$ mm. The operating frequency is 915 MHz. The maximum read-range for this design is about 11 cm and -10 dB bandwidth is from 820 MHz to 1050 MHz.

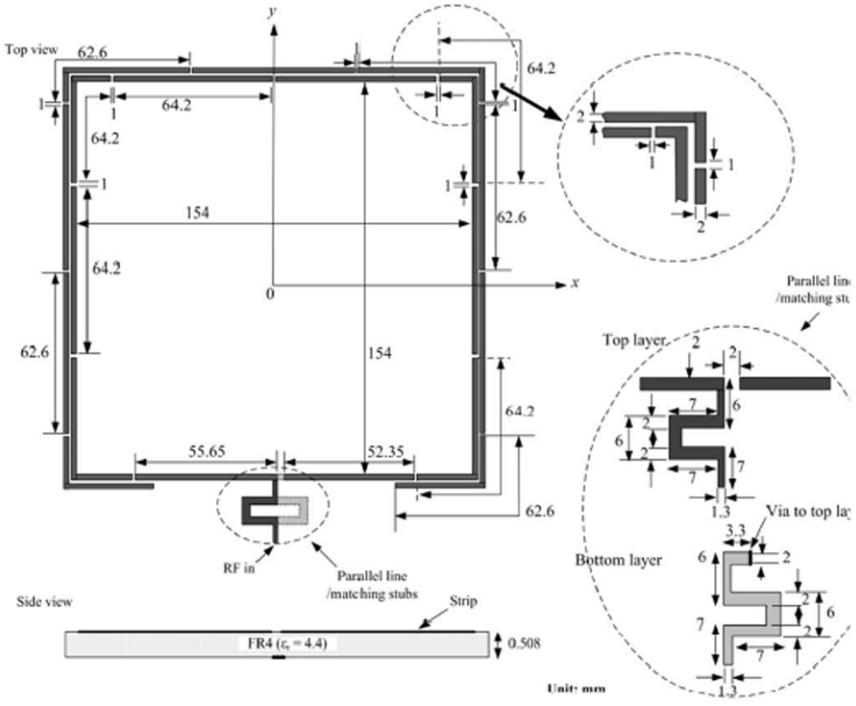

Figure 4.6: Segmented Loop Antenna Review 3 [24].

Here is another segmented loop antenna [29] designed for analysis of far-field radiation pattern. The purpose of segmentation here is also to make the current and its phase distribution uniform for larger loop antenna so that it behaves like an electrically small antenna so as to obtain the omnidirectional radiation pattern. The segments are on top and bottom of the substrate alternatively with some area overlapped to introduce capacitive effect. This loop structure is mentioned because this thesis implements the similar structure for near-field operation.

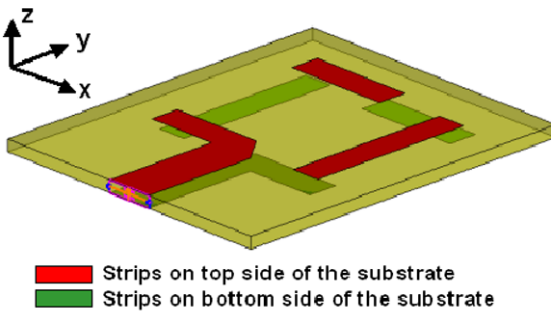

Figure 4.7: Segmented Loop Antenna Review 4 [29].

A variable pitch one arm spiral design [30] can also be used for RFID near-field application. This element is mounted about 20 mm above the ground plane. This antenna reads tags over an area of around 200 mm × 200 mm and it can read 90% of the tags up to 50 mm for all positions and orientations.

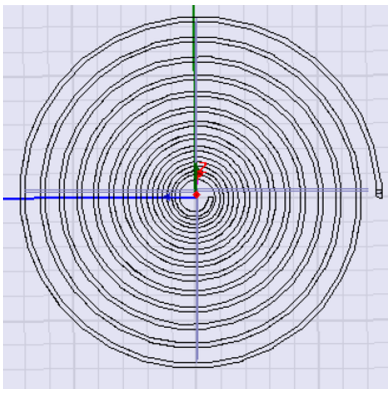

Figure 4.8: Spiral Near-Field Antenna [30].

4.3 Far Field Operations

The information exchange between reader antenna and tag in far-field is via electromagnetic wave. The read-range of the far-field reader antennas depends on the gain and polarization of the antenna. The orientation of the antennas should be such that both antennas have the same polarization. The commonly used reader antennas are the patch antennas. Therefore, we focus here on the patch antennas.

4.3.1 Antenna Parameters and Properties

It is useful to explain some basic parameters of antennas before going to design techniques.

Radiation Pattern: It is defined as "a mathematical function or a graphical representation of the radiation properties of the antenna as a function of space coordinates". If electric or magnetic field is used, then it is called field pattern. If power

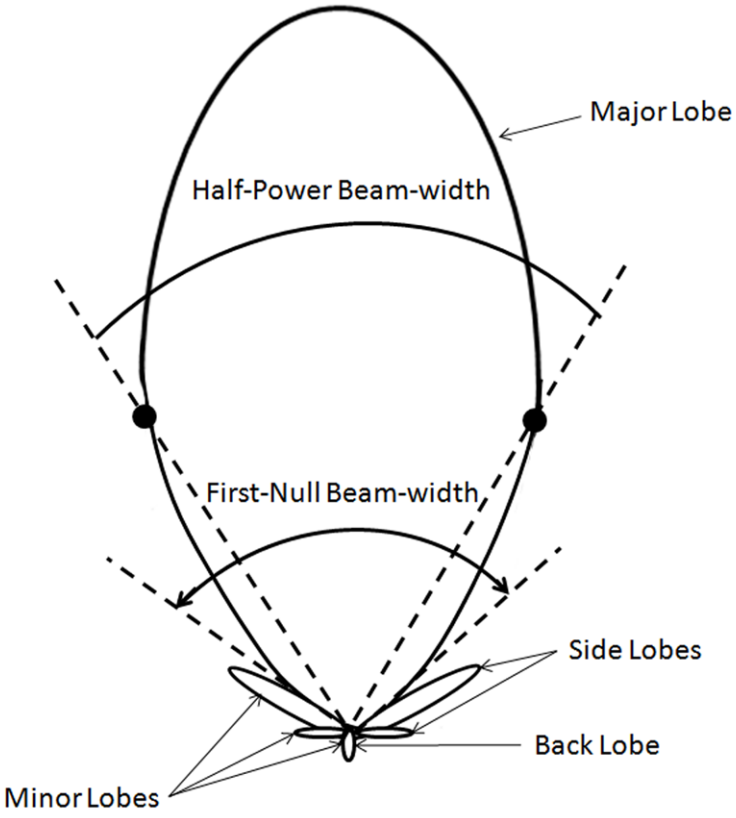

Figure 4.9: Radiation Pattern of an Antenna [31].

density is used, then it is called the power pattern [31].

Power pattern is shown in the Figure 4.9. It shows different kinds of lobes. Main lobe characterizes the direction of maximum radiation. All other lobes are minor lobes which represent radiation in undesired directions and should be minimized. Normalized power pattern is expressed as

$$P_n(\theta, \phi) = \frac{S(\theta, \phi)}{S(\theta, \phi)_{\max}} \text{ (Dimensionless)}, \tag{4.2}$$

where $S(\theta, \phi)$ is poynting vector ($\mathrm{W/m^2}$) and $S(\theta, \phi)_{\max}$ is the maximum value of $S(\theta, \phi)$.

Beamwidth: In a plane containing the direction of the maximum of a beam, the angle between the two directions in which the radiation intenisty is one-half value of the beam as shown in the Figure 4.9 is referred to as the half-power beamwidth (HPBW) [31]. There is another beamwidth called first-null beamwidth (FNBW) which is defined as the angular separation between the first nulls of the pattern.

Beam Area or Beam Solid Angle: An area of the surface of a shpere subtends

an angle at the center which is known as the solid angle Ω. The total solid angle subtended by the whole surface of the sphere is 4π steradians (sr) or square radians.

Radiation Intensity: The power radiated from an antenna per unit solid angle is called the radiation intensity U (W/sr). The normalized power pattern can also be expressed in terms ot radiation intensity as

$$P_n(\theta, \phi) = \frac{U(\theta, \phi)}{U(\theta, \phi)_{\max}} \text{ (Dimensionless).} \tag{4.3}$$

Directivity: It is defined as the ratio of the radiation intensity in a given direction from the antenna to the radiation intensity averaged over all directions [31].

$$D = \frac{U}{U_0} = \frac{4\pi U}{P_{\text{rad}}} \text{ (Dimensionless),} \tag{4.4}$$

where U_0 is radiation intensity of an isotropic radiator (W/sr) and P_{rad} is the total radiated power (W).

Antenna Efficiency: All the power fed to the antenna may not be radiated. There occur reflections and losses (conduction and dielectric) in the antenna system which make the efficiency less than 1. The total efficiency of an antenna is formulated as

$$e_0 = e_{\text{r}} e_{\text{c}} e_{\text{d}} \text{ (Dimensionless),} \tag{4.5}$$

where e_{r} is the reflection or mismatch efficiency (dimensionless), e_{c} is the conduction efficiency (dimensionless), and e_{d} is the dielectric efficiency (dimensionless). Normally, e_0 is expressed as $e_0 = e_{\text{r}} e_{\text{cd}}$, where $e_{\text{cd}} = e_{\text{c}} e_{\text{d}}$ is used to relate the gain and directivity.

Gain: Gain (G) of an antenna in a given direction is defined as the ratio of the intensity in that direction to the radiation intensity that would be obtained if the power accepted P_{in} by the antenna were radiated isotropically. i.e.,

$$G(\theta,\ \phi) = 4\pi \frac{U(\theta,\ \phi)}{P_{\text{in}}} \text{ (Dimensionless).} \tag{4.6}$$

The total radiated power (P_{rad}) is related to the total input power (P_{in}) by

$$P_{\text{rad}} = e_{\text{cd}} P_{\text{in}}. \tag{4.7}$$

Gain does not accomodate impedance mismatches and polarization mismatches.

Therefore,

$$G(\theta,\ \phi) = e_{\text{cd}}\left[4\pi\frac{U(\theta,\ \phi)}{P_{\text{rad}}}\right] = e_{\text{cd}}D(\theta,\ \phi). \tag{4.8}$$

Polarization: It can be defined as the orientation of the electric field at a specified point as the function of time. It is the special property of the plane wave radiated by an antenna. In a given +z-direction of propagation, the plane wave consists of electric field and magnetic field varying along x- and y- axes with respect to time. Magnetic field and electric field are perpendicular to each other. Therefore, it is suffiecient to explain the behaviour of the electric field. Suppose, the plane wave traveling along +z-direction consists of the following E-field components:

$$E_x = E_1\sin(\omega t - \beta z), \tag{4.9}$$

$$E_y = E_2\sin(\omega t - \beta z + \delta), \tag{4.10}$$

where E_1 is the electric field in x-axis, E_2 is the electric field in y-axis, and δ is the phase difference between E_x and E_y. The instantaneous total electric field vector $\overrightarrow{E}$ is

$$\overrightarrow{E} = \hat{x}E_1\sin(\omega t - \beta z) + \hat{y}E_2\sin(\omega t - \beta z + \delta). \tag{4.11}$$

Derivation from this equation leads to the expression of an ellipse. There are three types of polarization: linear, circular, and elliptical. Linear and circular polarizations are the special cases of the elliptical polarization.

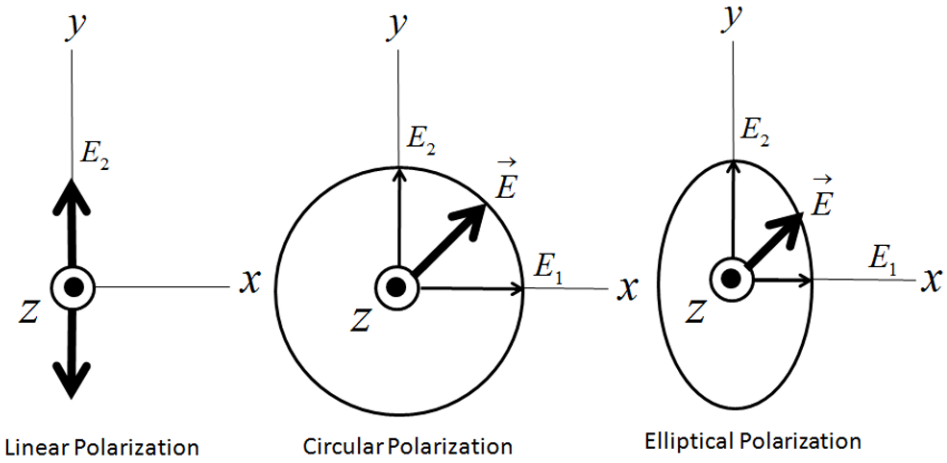

Figure 4.10: Antenna Polarization [32].

If E_1 or E_2 is zero then the wave is linearly polarized in y- or x-axis. If $\delta = 0$ and $E_1 = E_2$, the wave is again linearly polarized but it is tilted at 45°. If $E_1 = E_2$ and $\delta = \pm 90°$, the wave is circularly polarized. If the tip of the electric field vector $\overrightarrow{E}$ rotates in a clockwise fashion (for wave receding the observer), it is called the

right-hand polarization (occurs when $\delta = -90°$), otherwise it is left-hand polarization (occurs when $\delta = +90°$).

4.3.2 Patch Antenna Design Technique

The microstrip patch antennas can be in different shapes such as square, rectangular, circular, and so on. A microstrip patch antenna consists of a very thin metallic patch placed above a ground plane with separation of about $0.003\lambda \leq h \leq 0.05\lambda$. The maximum radiation is made in the direction normal to the patch with proper design. The length of a rectangular patch is usually $\lambda/3 < L < \lambda/2$. Substrate is used in between patch and the ground plane. There are different substrates available with different dielectric constants. The substrate with lower value of permittivity and higher thickness provides the better performance in terms of efficiency and bandwidth [31].

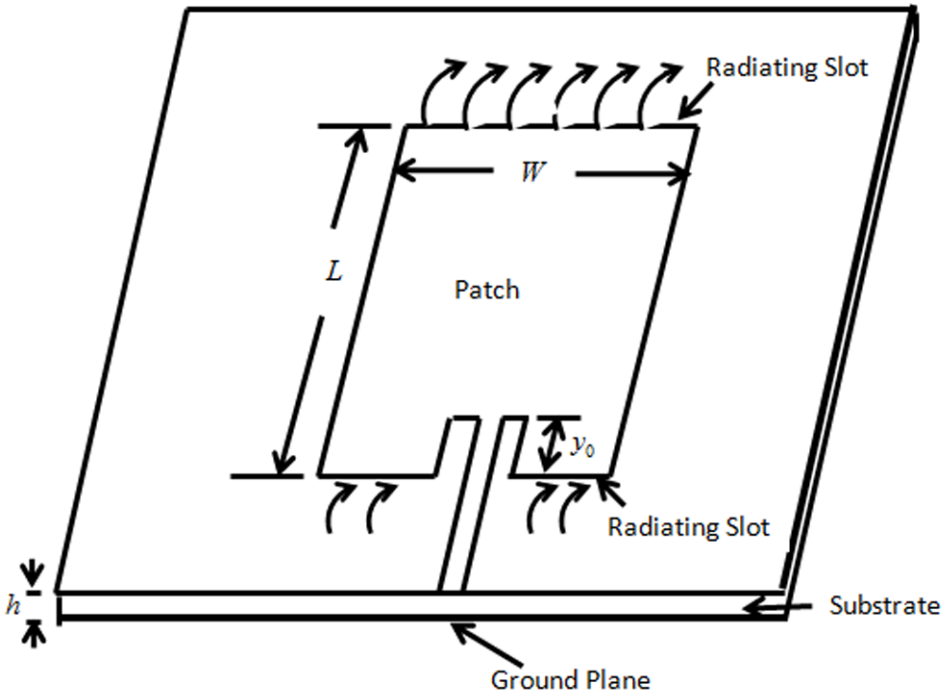

Figure 4.11: Rectangular Patch Antenna with Inset Microstrip Line Feed [31].

In this section we will discuss about the transmission-line model of a rectangular patch antenna. This model represents the rectangular microstrip antenna as an array of two radiating slots, separeted by a low impedance transmission line of certain length. Since the width and the length of the patch are finite, the fields at the edges suffer from fringing effect. The field exists outside the dielectric thus causing a change in the effective dielectric constant. The amount of fringing depends

on length and width of the patch, height and dielectric constant of the substrate. Though in small quantity, it should be considered in design because it affects the resonance frequency of the antenna. The fringing at the edges as shown in figure increases the effective length of the patch.

For $W/h > 1$, the effective dielectric constant is given by

$$\epsilon_{\text{reff}} = \frac{\epsilon_{\text{r}} + 1}{2} + \frac{\epsilon_{\text{r}} - 1}{2} \left[1 + 12 \frac{h}{W} \right]^{-1/2}. \tag{4.12}$$

The effective length due to fringing effect is formulated as

$$L_{\text{eff}} = L + 2\Delta L, \tag{4.13}$$

where ΔL is given by

$$\Delta L = 0.412 \frac{(\epsilon_{\text{reff}} + 0.3)(\frac{W}{h} + 0.264)}{(\epsilon_{\text{reff}} - 0.258)(\frac{W}{h} + 0.8)} h. \tag{4.14}$$

For effiecient radiation, width of the patch should be

$$W = \frac{c}{2 f_{\text{r}}} \sqrt{\frac{2}{\epsilon_{\text{r}} + 1}}. \tag{4.15}$$

The actual length of the patch is determined by

$$L = \frac{c}{2 f_{\text{r}} \sqrt{\epsilon_{\text{reff}}}} - 2\Delta L. \tag{4.16}$$

For the patch antenna with microstrip feedline, the resonant input resistance can be changed for the input matching by using an inset feed as shown in the figure. The maximum value occurs at the edge of the slot ($y_0 = 0$) where the voltage is maximum and the current is minimum. The minimum value i.e., 0 occurs at the center of the patch ($y_0 = L/2$) where the voltage is zero and the current is maximum.

5. SEGMENTED LOOP ANTENNA WITH PATCH

Loop antenna is normally used for near-field communication. Though it has certain radiation pattern, it is not used for far-field operation due to the fact that it does-not radiate toward the region of interest. There are some patent designs [33], [34] for RFID reader antenna reading both near-field and far-field tags. The near-field and far-field performances with these designs are either not in the same direction or not at the same frequency. Since we are aiming to get both the near-field and the far-field performances at UHF and in the same direction, the segmented loop is the basic requirement and some modifications or additional structures are needed for far-field. While designing an antenna, the size also should be considered in high priority.

Top to bottom coupled segmented loop has been used for near-field reading. There can be implemented different kinds of designs [35], [36], [37], and [38] for far-field radiation. But, for making the design simple, a normal patch antenna [31] has been used inside the loop for far-field operation. Theoretically, the copper plate should not affect the magnetic field passing through it and this is the reason of motivation to use the patch antenna inside the loop. The size of the antenna is not affected by the introduction of patch because it has been designed such that it fits inside the loop.

5.1 Design Process

Loop antenna is designed in such a way that the current flow through it is unidirectional. At LF/HF systems, the wavelength is large and the physically large loop is still electrically small which is very less than the operating wavelength. In this case, the current flows in the same direction through the whole loop. Current reverses its direction after every half wavelength demanding the loop size less than half wavelength for unidirectional flow of current. For uniform distribution of current along the loop, it should be less than half wavelength. It is said that the optimal length of the segment should not exceed one tenth of the operating wavelength [25].

At UHF band, the wavelength is so small that quarter wavelength is physically very small and the reader antenna with this size of loop is of no use. The loop size

should be comparable to the wavelength to get the optimal size of the antenna. The physically large loop can be made electrically small by segmenting the loop into different pieces and capacitors are introduced in between the segments.Normally, the segments should be less than quarter wavelength. The length of the loop gives the inductance and the added capacitors try to nullify the inductive effect to get the resonance at the desired frequency. The capacitor values in between the segments depend on the length and width of the loop.

Generally, lumped components of capacitors are not used in such designs because of unavailability of required values and tolerance issues. The capacitive effect is produced by using the coupling mechanism between the segments. There can be implemented different designs for coupling such as side by side coupling and top to bottom coupling or both. We have used top to bottom coupling in our design since the capacitance can be varied largely by adjusting the width of the conducting strips.

A normal patch antenna has been inserted inside the loop to add the far-field performance. It is really challenging to merge two different types of antennas since it is highly probable of interfering each other. The loop antenna provides not only the near-field magnetic field but also the far-field radiation pattern which can affect the radiation by the patch antenna. Similarly, the magnetic field by loop may be affected by the current distribution over the patch or the presence of patch and ground plane themselves. And, another challenge is to tune to the right frequency with sufficient bandwidth.

5.2 Antenna Structure

The final simulated structure of the antenna is shown in the Figure 5.1. Since the antenna has print on both the sides, different colour has been used to distinguish different parts. Figure 5.2 gives the detail dimensions of the top and bottom views. Red colour has been used to show the copper parts on the top side, black the bottom side, orange the copper parts of the feed system, and pink the substrate. The overall size of the antenna is 17.4 cm $\times$ 18.4 cm and is oriented on xy-plane. The width of all the loop strips and the feed lines is 8 mm. The region of operation is toward +z-axis.

There are eight segments in the loop; four on the top and four on the bottom. Some portion of the top and bottom segments are overlapping each other for producing distributed capacitors. The resonance frequency depends on the width and the length of the loop segments and the overlapping region. The perimeter of the loop is 616 mm. This design is made for the UHF RFID frequency range of European band i.e., 865 MHz to 868 MHz. The center frequency chosen is 866.5 MHz which gives

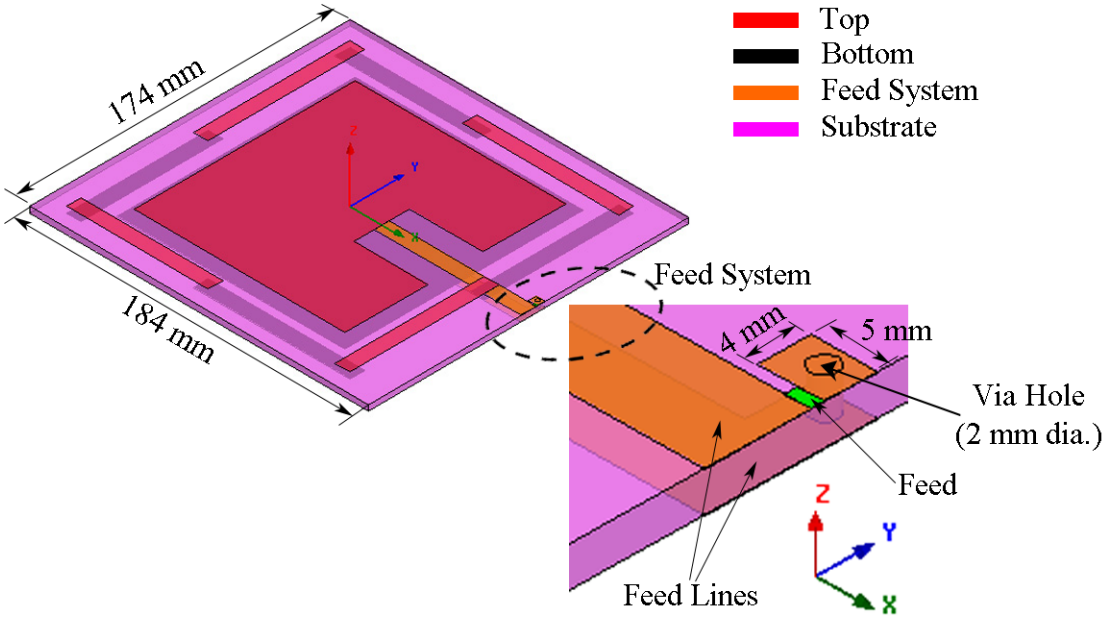

Figure 5.1: Antenna Structure for Loop Antenna with Patch.

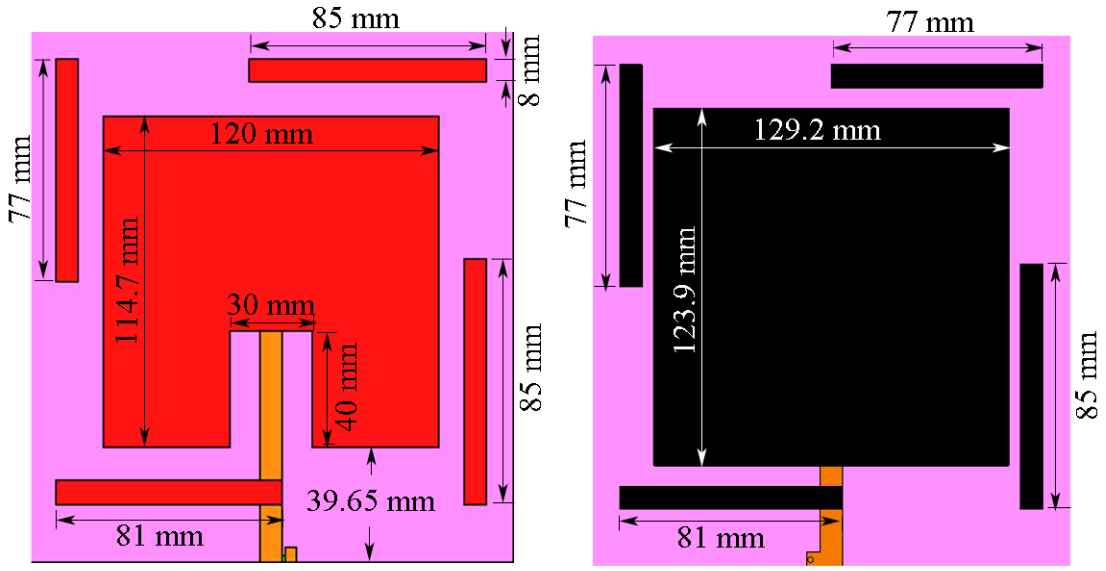

Figure 5.2: Top and Bottom View of the Antenna.

the wavelength (λ) of 346 mm in free space. The loop size is therefore 616/346 = 1.78 λ. The substrate used here is Rogers RT 5880 with relative permittivity of 2.2 and the thickness of 3.175 mm. The ground plane is slightly larger than the patch. It would have been better to make the ground plane even bigger for the backlobe reduction and the gain enhancement. But, it is not possible here because the loop restricts the size of both the patch and the ground plane. There is compromise also

with the separation between them. The inset type microstrip feed mechanism has been used here for simplicity. The ground signal is taken to the top by using the conductor through VIA hole so that a simple SMA connector can be used to feed the antenna.

5.3 Simulations Results

The Ansoft HFSS (High Frequency Structure Simulator) software [39] has been used for simulations. This software can be used for 3D full-wave electromagnetic field simulation and is able to run high-frequency and high-speed designs. HFSS is based on the finite element method (FEM) algorithm and implements different electromagnetic theories as explained in the second chapter "Electromagnetic Basics".

5.3.1 S_{11} and Input Impedance

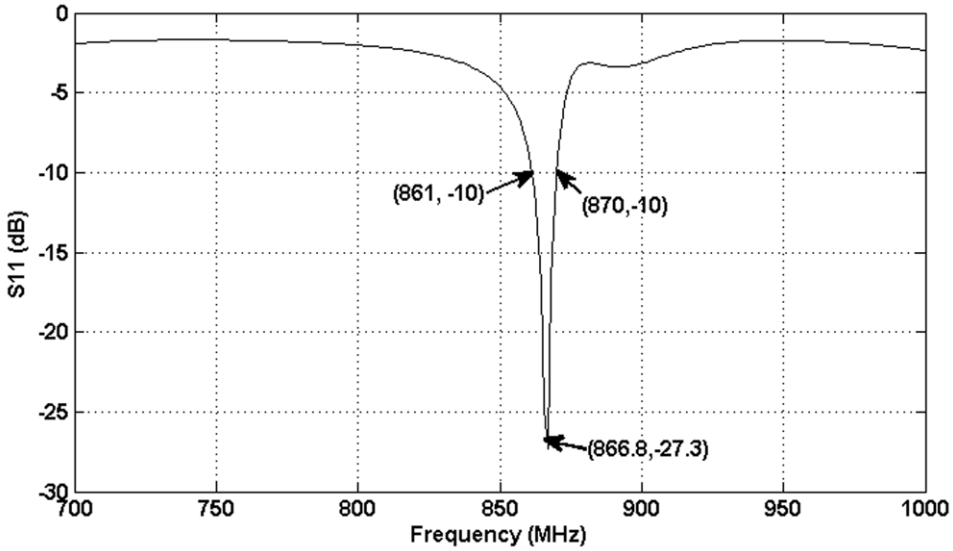

Figure 5.3: Simulated S_{11}.

Figure 5.3 is the simulated S_{11} of the antenna design. If we consider that -10 dB of S_{11} is sufficient for operation, then the bandwidth is available from 861 MHz to 870 MHz which covers the European band of 865 MHz to 868 MHz. The antenna resonates at 866.8 MHz with minimum S_{11} of -27.3 dB. It is clear from the figure that the value of S_{11} is low enough at our desired frequency of 866.5 MHz.

The antenna is designed for the source impedance of 50 Ω; the input impedance should have real part of 50 Ω and imaginary part of 0 Ω for the perfect matching condition. However, the values close to them are sufficient for the required return loss or S_{11}. The Figure 5.4 depicts the input impedance of the antenna. The real

part is 51.3 Ω and the imaginary part is 4.18 Ω at the resonant frequency of 866.8 MHz.

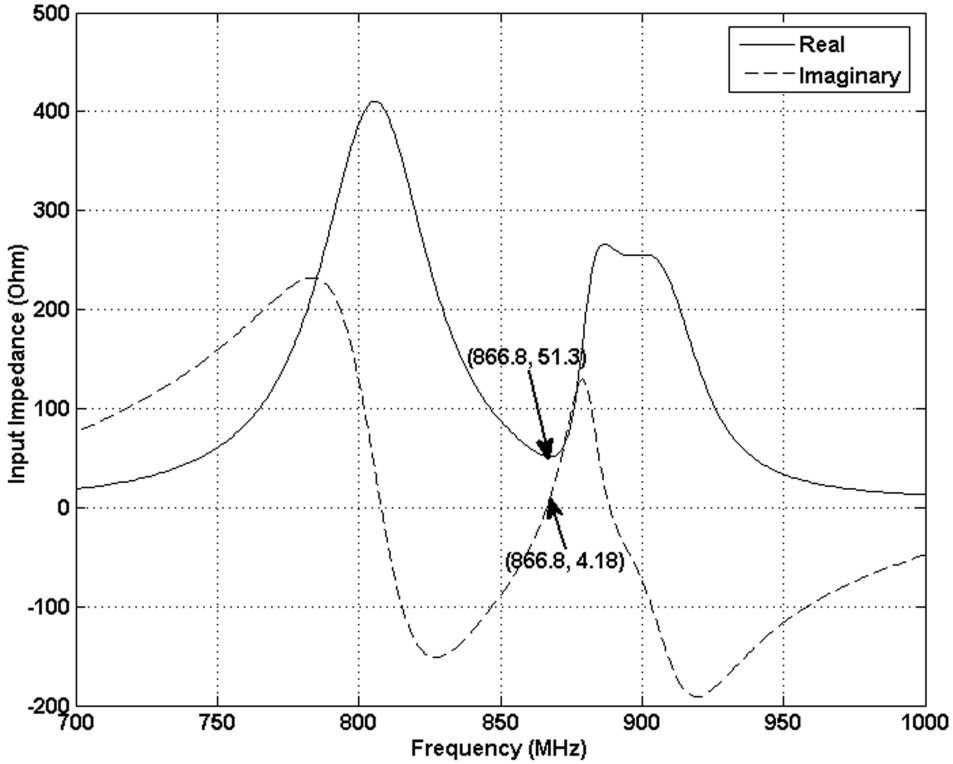

Figure 5.4: Simulated Input Impedance.

5.3.2 Current and Magnetic Field Distribution

Since the loop is segmented for making it electrically small, the current is expected to flow in a single direction. And, the uniform distribution of magnetic field on the xy-plane is required to have good near-field performance all around the surface of the antenna on the xy-plane.

The current distribution along the segmented loop is almost unidirectional thereby producing almost uniform magnetic field on the xy-plane. The plane for plotting the magnetic field is 20 mm away from the antenna surface.

The uniformity of the magnetic field distribution can be viewed closely by plotting the field along the lines along x-axis and y-axis inside the interrogation zone as shown in the Figure 5.6. The lines are 20 mm above the antenna surface. The magnetic field variation is less than 10 dB.

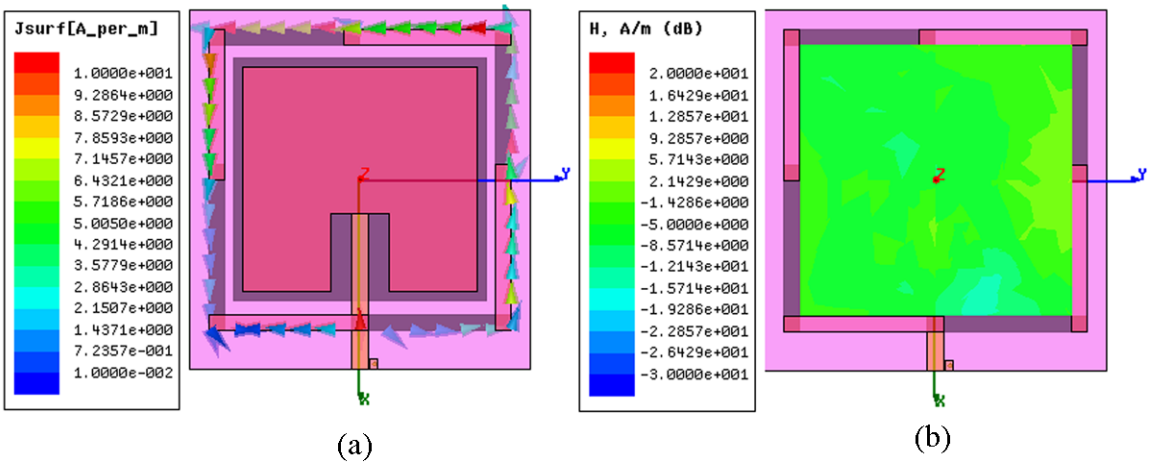

Figure 5.5: (a) Current Distribution, and (b) Magnetic Field Distribution.

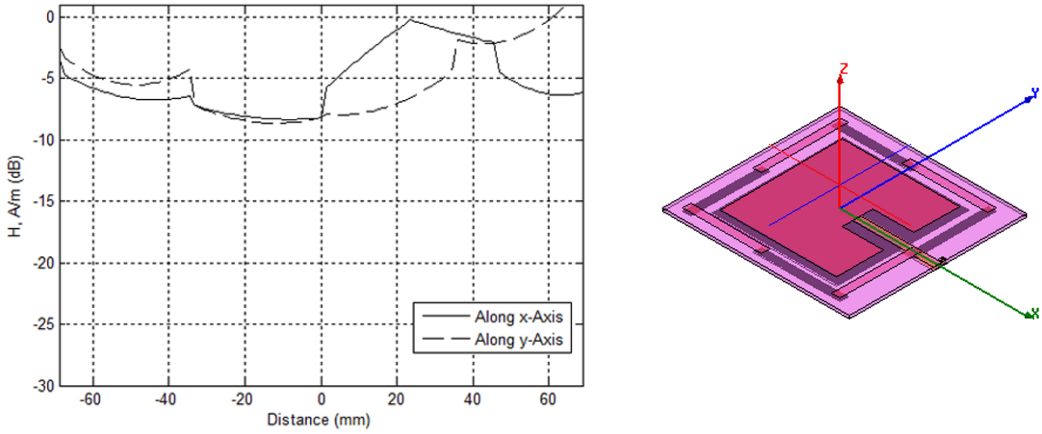

Figure 5.6: Magnetic Field Distribution Along x-Axis and y-Axis.

5.3.3 Realized Gain

The patch antenna radiates along z-axis with linear polarization. The E-Plane lies on the xz-plane whereas the H-Plane lies on the yz-plane. Since the ground plane is restricted in size, the ratio between major lobe and minor lobe radiation is not large. This makes the antenna able to read the tags behind it up to certain distance which is the undesired operation.

The Figure 5.7 shows the radiation pattern of the realized gain which has the maximum gain of slightly greater than 5 dBi. The radiation is almost along +z-axis which is the expected performance for far-field. The realized gain on xz- and yz-planes are shown in the Figure 5.8 for clear view of the radiation pattern.

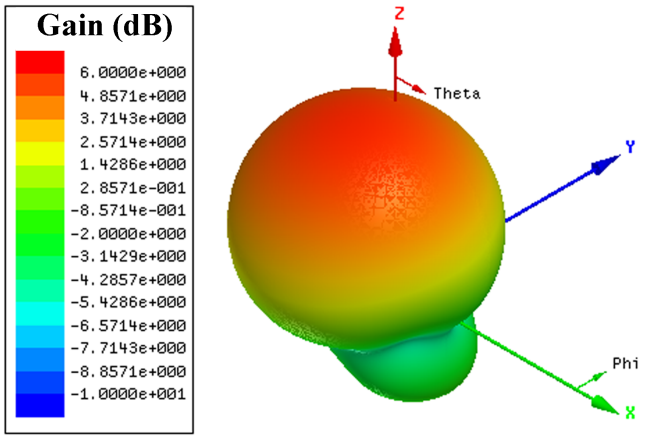

Figure 5.7: Realized Gain in 3D.

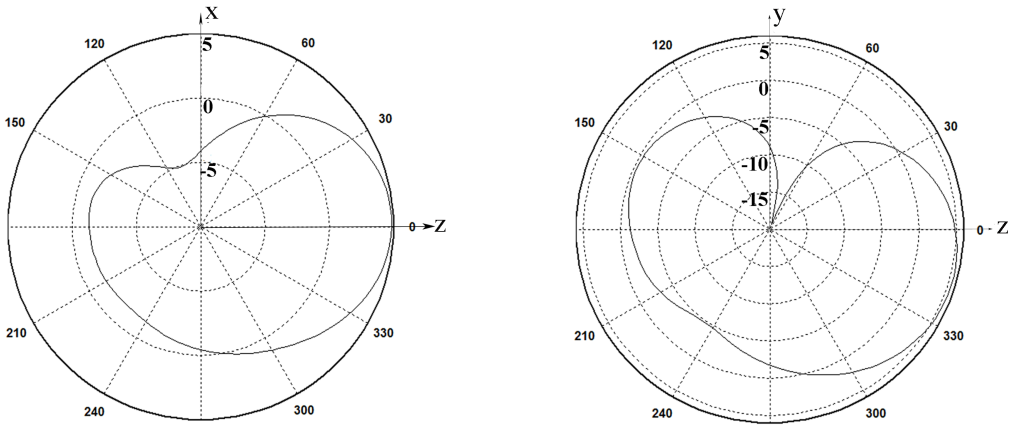

Figure 5.8: Realized Gain on xz- and yz-Planes.

5.4 Antenna Fabrication

Normally, it is difficult to fabricate the double sided structure. The slight shift of the position of any layer may alter the performance drastically. Therefore, great care must be taken during fabrication. There are two methods of fabricating an antenna: etching and milling. We have used doubled sided Rogers RT 5880 substrate for our antenna design. This substrate doesnot have photoresist layer on top of the copper plates. We have to add the photoresist layer by using the chemical so that it can be printed with the help of photolithography before etching. The antenna size is so huge that this process becomes too much complicated and the milling machine is used instead. The machine drills the copper out from the unnecssary parts. The substrate should be fixed properly in the machine and there should not be shift in the coupling region between top and bottom strips.

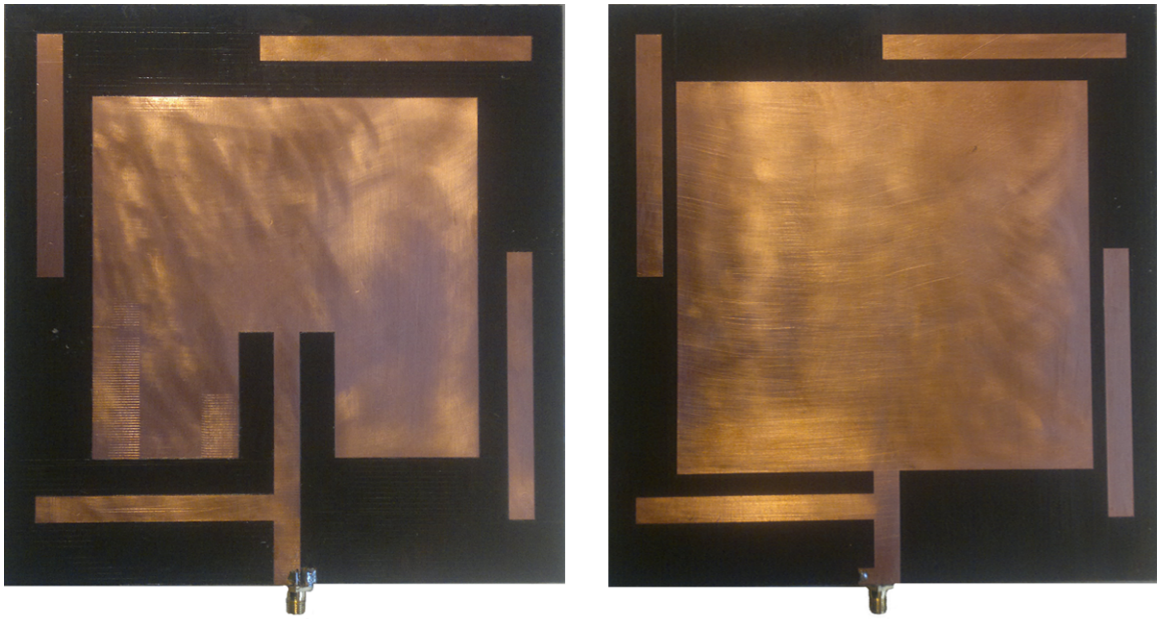

Figure 5.9: Prototype: (a) Top View, and (b) Bottom View.

The Figure 5.9 is the prototype of the antenna design. This shows the top and bottom view of the prototype.

5.5 Measurements Results

5.5.1 S_{11} and Input Impedance

S_{11} and input impedance of the fabricated prototype are measured by using the vector network analyzer (VNA). The simulated results are also plotted in the same figure to ease the comparison. The Figure 5.10 shows the S_{11} curves for both the simulated and the measured results. The solid line is used for simulations and the dotted line for measurements. There is shift in the resonance frequency to the right by around 3 MHz as seen from the Figure 5.10. Normally, the simulations results do not match with the measurements results perfectly due to different practical issues. The bandwidth of the prototype is from 864 MHz to 873 MHz which still covers the required European band.

The Figure 5.11 and 5.12 give the real part and the imaginary part respectively of the input impedance for simulation and measurement. The measured real part is almost 50 Ω and the imaginary part almost 0 Ω at the resonance frequency.

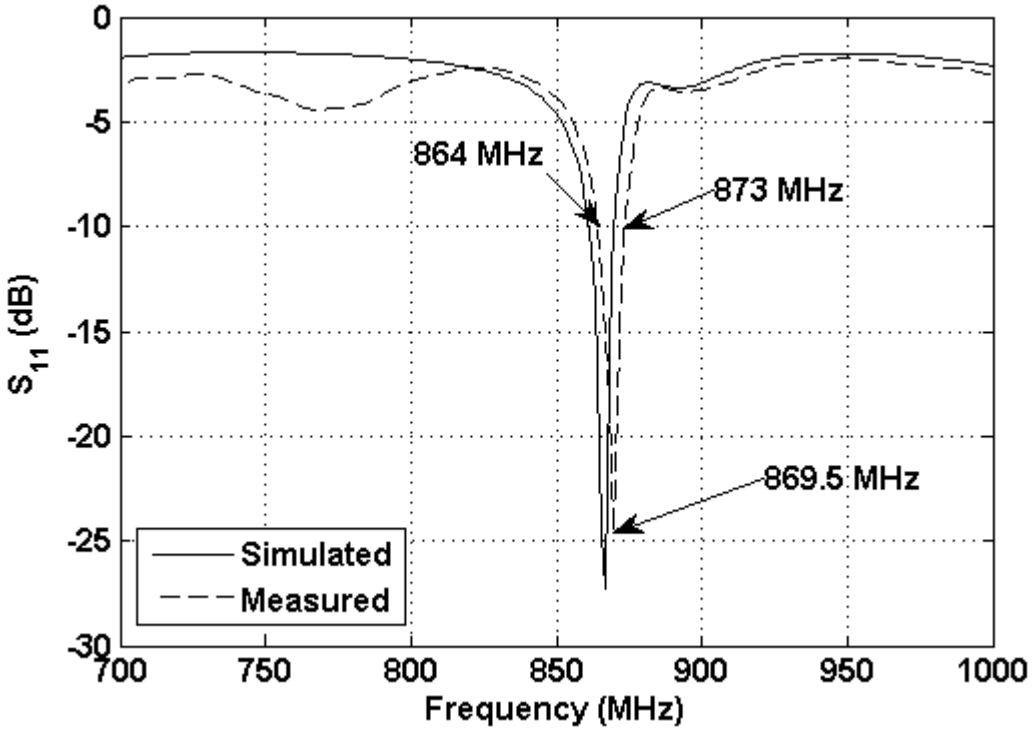

Figure 5.10: Measured and Simulated S_{11}.

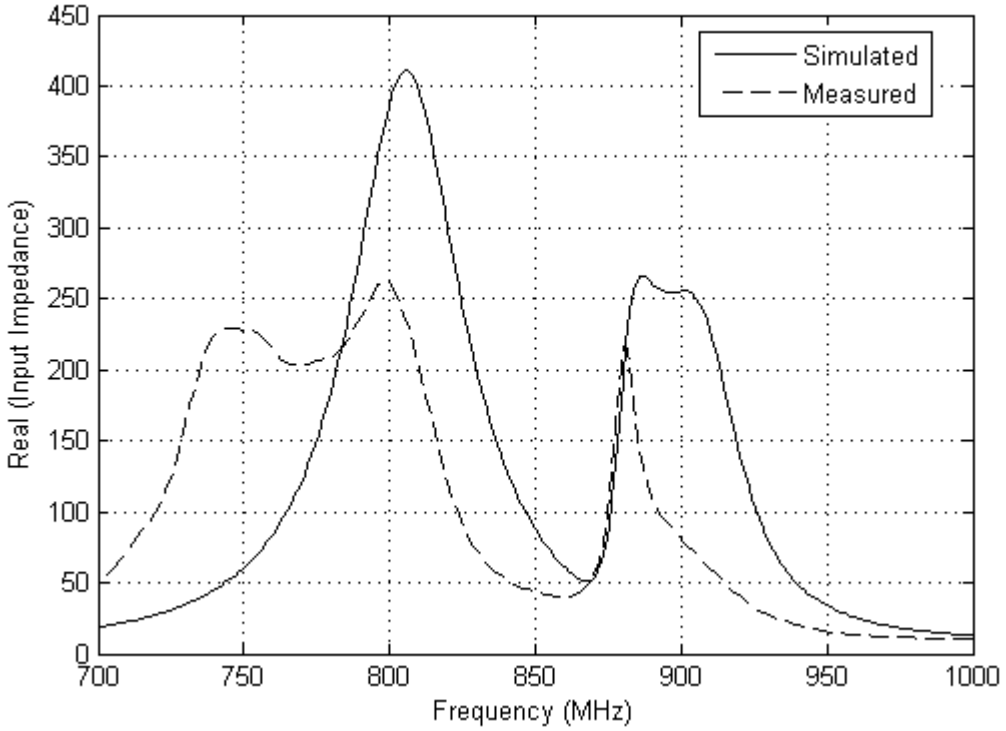

Figure 5.11: Real Part of Input Impedance for Simulation and Measurement.

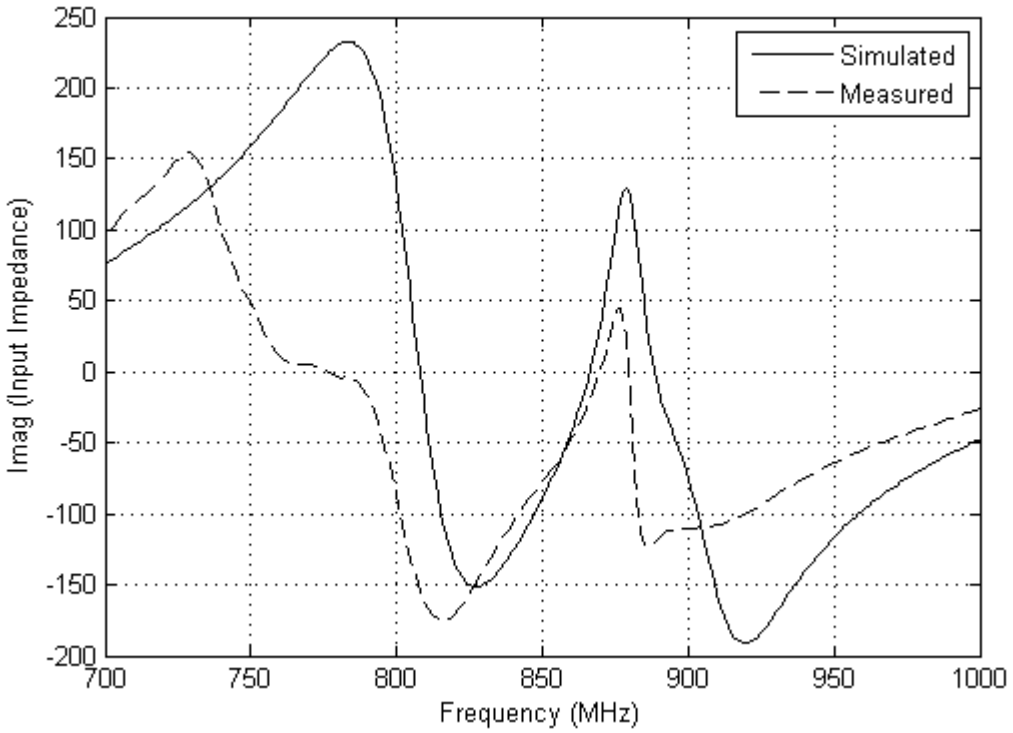

Figure 5.12: Imaginary Part of Input Impedance for Simulation and Measurement.

5.5.2 Realized Gain

The radiation pattern of the fabricated antenna is measured in the Satimo Star Lab. The radiation patterns for simulations and measurements look similar. But, the gain is slightly less in the measured pattern. The maximum measured gain is about 4 dBi. It is clear from the figures that the back lobe radiation has gain more than -5 dBi. This gives the ratio of major lobe to back lobe less than 10 dB. It is good to have this ratio very high to prevent the reading of tags in the back side of the antenna. However, there is compromise in the size of the ground plane and the width of the substrate to reduce the back lobe radiation. The Figure 5.14 is the 3D view of the measured radiation pattern.

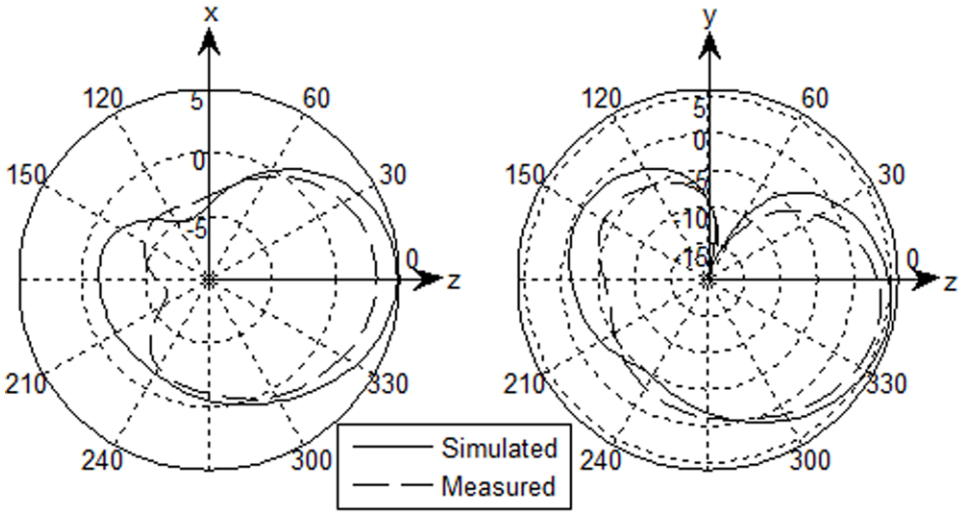

Figure 5.13: Radiation Pattern on xz- and yz-Planes.

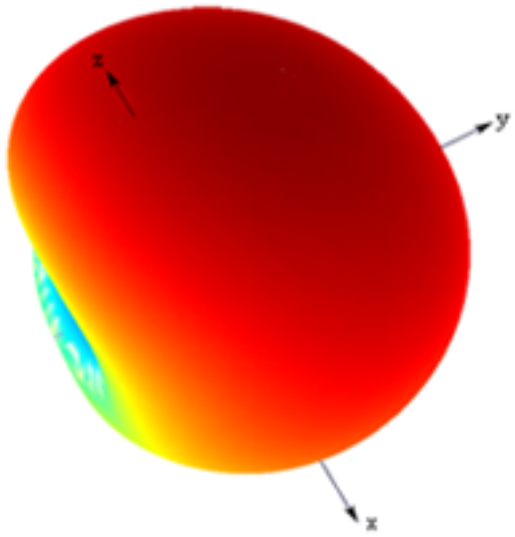

Figure 5.14: Radiation Pattern in 3D.

5.6 Read-Range Measurements

Read-range is an important characteristic of the RFID system. It depends on several factors such as gain, polarization, and relative position of the reader antenna and the tag antenna, sensitivity of reader unit and tag IC, transmitted power, and the surrounding environment. Measurements are taken in different scenarios and with different tags. The reader unit used is from Alien Technology [40]. The measurement set up is shown in the Figure 5.15.

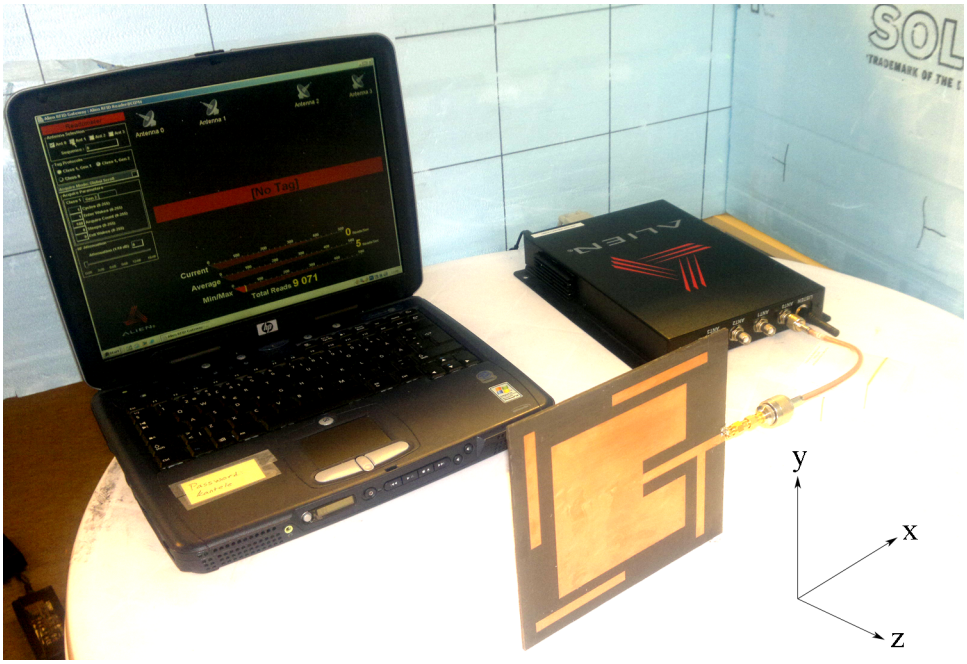

Figure 5.15: Measurement Set Up.

5.6.1 Near-Field Measurements

Since the reader antenna is loop type for near-field operation, the tag antenna also should be loop type for the effective magnetic coupling between them. The near-field tags are normally used in small objects and hence should be small. The button type tag of around 8 mm diameter is commonly used for near-field application. The measurements are taken with tags in different orientations.

When tag is parallel to the antenna plane, the read-range performance is different at different positions. It does not read from small portion of the center region. The maximum read-range in this orientation is 9 cm. Since the antenna does not have uniform read-range performance, the maximum read-range (in cm) at certain locations are marked over the antenna as shown in the Figure 5.16. The near-field tag used in this measurement is also shown in the same figure.

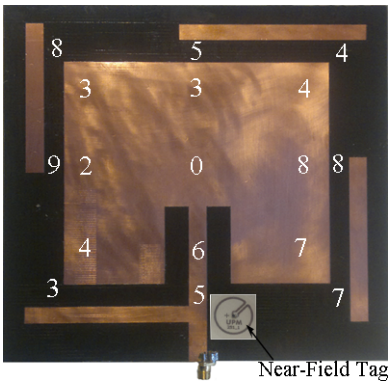

Figure 5.16: Near-Field Performance of the Antenna.

When tag is positioned on the xz-plane, the reader antenna reads the tag up to 5 cm more uniformly than the previous orientation from all the parts in the interro-

gation zone. After this range, the antenna does not read for about 11 cm and again starts reading for couple of centimeters. This observation is somehow strange and unexpected.

The observation is taken with tag on yz-plane also. But, the performance is very poor.

5.6.2 Analysis for Near-Field Performance

The expectation from the antenna is to read the tags from all over the interrogation zone when placed parallel to its surface which should be the case for any loop antenna. Though our antenna is reading near-field tags from the regions nearby the loop as seen in the Figure 5.16, the performance is null at the center region which should be analyzed properly. In the simulations, the magnetic field distribution is almost uniform and our expectation should therefore be valid. However, it's better to observe the field components separately because z-component is the field responsible for near-field performance when tag is parallel to the reader antenna.

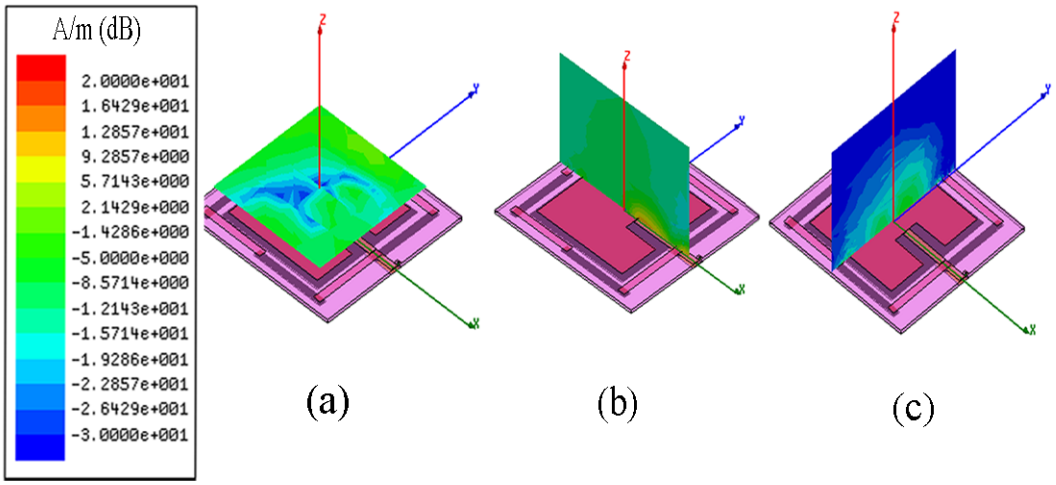

Figure 5.17: Different Field Components: (a) z-Component at 20 mm Away, (b) y-component for Plane of 10 cm Height, and (c) x-component for Plane of 10 cm Height.

The simulations results for different magnetic field components are shown in the Figure 5.17. Though the resultant magnetic field as given in the Figure 5.5(a) is uniform, the z-component alone is not. This component is extremely weak at certain locations in the center region of the antenna as found in the Figure 5.17(a). This might be the reason of not detecting the tag from some center regions.

While examining the y-component on the xz-plane, the field strength is pretty ok

which should be the reason for reading the tags on the xz-plane. This field component might have come from the current distribution of the patch. The current flows on the patch along x-axis which can result the magnetic field along y-axis.

The x-component of magnetic field distribution on yz-plane is shown in the Figure 5.17(c). The field is very weak indicating the poor near-field performance of the antenna with this orientation.

The z-component of the magnetic field along x-axis and y-axis at 20 mm above the antenna in the interrogation zone is displayed in the Figure 5.18. It is clear from the figure that z-component of the field varies a lot and is very weak at the center. On the other hand, it is comparatively strong in the periphery thus giving the better reading performance.

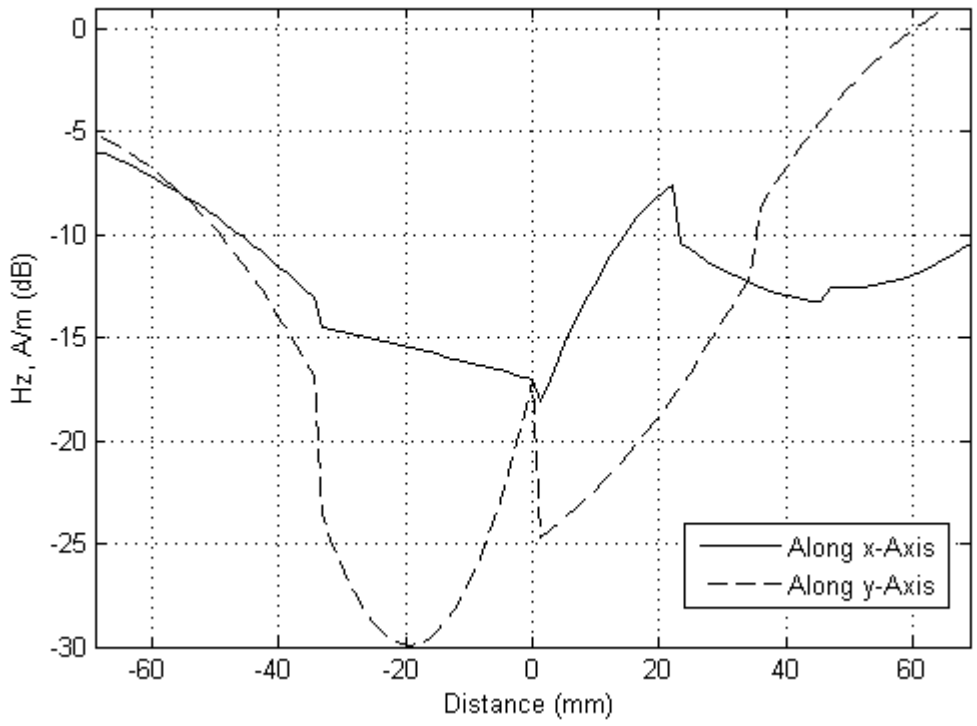

Figure 5.18: z-Component of Magnetic Field Along x-Axis and y-Axis.

5.6.3 Near-Field Measurements with Objects

The magnetic field is not much affected by the objects with higher permittivity. In practice, tags are attached on the objects and the motif of RFID system is to implement the technology such that the objects do not degrade the reading performance

too much. We have done some near-field measurements with the same tag attached on some objects. Tag is oriented parallel to the antenna.

This measurement is done to show that the near-field performance is not much affected by the objects containing liquids. The maximum read-range for all the objects shown in the Figure 5.19 is about 8 cm.

Figure 5.19: Different Objects for Near-Field Measurements.

5.6.4 Far-Field Measurements

Dipole type tags are normally used for the far-field operations. The proposed antenna is linearly polarized thus giving the better read-range only in one orientation or when both the reader antenna and the tag antenna are oriented in copolarization. The read-range depends not only on the orientation of the antennas but also on their types and gain and the objects on which tags are attached.

There are varieties of far-field tags available in the market. We have examined the read-range performance of the reader antenna with some of the commercial tags as shown in the Figure 5.20. Since the reader unit provides the maximum of 2 W ERP for the reader antenna with gain of 6 dBi and our antenna has gain of about 4 dBi, we do not need to attenuate the transmitted power of the reader unit. The maximum read-ranges of the reader antenna for different tags are listed in the Table 5.1.

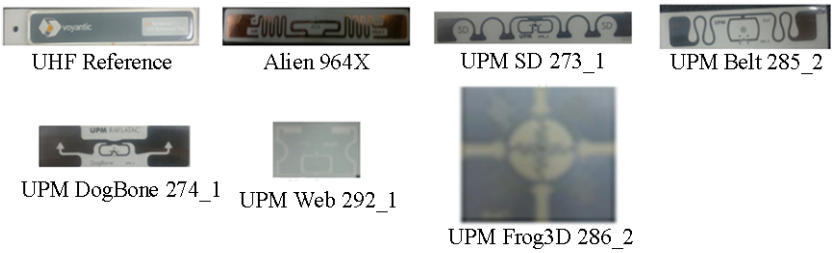

Figure 5.20: Far-Field Commercial Tags [41], [42], [43].

Table 5.1: Read-Range with Different Tags.

No.	Tag	Read-Range (m)
1	UHF Reference	>5
2	Alien 964X	>5
3	UPM SD	>5
4	UPM Belt	3.5
5	UPM DogBone	2
6	UPM Web	2
7	UPM Frog3D	2

5.6.5 Far-Field Measurements with Objects

The far-field reading performance is greatly affected by the metal and liquid objects for normal tags. When a metal piece exists at a certain distance from the antenna, it changes the behaviour of the antenna in a large degree [44]. The performance varies from object to object depending on its nature and type. We have used UPM SD tag as reference. The purpose of such measurements is to show how the read-range alters with the use of objects.

Figure 5.21: Far-Field Read-Range with Different Objects.

The read-range for different objects are marked on the respective objects as given in the Figure 5.21. If the objects were water bottles and metallic cans, the read-range would have been negligibly small.

6. SEGMENTED LOOP ANTENNA

The segmented loop antenna with patch works for both the near field and far field. The near-field performance is not uniform; the small region in the center does not read the near-field tag whereas the far-field performance is satisfactory. It is obvious that the patch structure is affecting the near-field performance. In fact, the loop antenna also radiates and the loop segments connected to the source may act as a dipole. Therefore, we may achieve both the near-field and the far-field operations from the loop antenna without any far-field structure.

6.1 Antenna Structure

The design procedure is the same as mentioned in the first design. The size of the antenna is different due to the resonance issue. The main difference is the absence of patch and ground plane in the new design.

The detail and final dimensions of the antenna are shown in the Figure 6.1 and 6.2. The overall size of the antenna is 143.5×133.5 mm^2. The loop is partitioned into eight segments each with length either 56.75 mm or 62.75 mm and width 6 mm. The overlapping area is 6 mm $\times$ 6 mm between each consecutive segments. The substrate used here is again Rogers RT 5880 with relative permittivity of 2.2 and height of 3.175 mm. The resonance frequency can be changed by changing the length and width of the copper strips and also the overlapping areas. The input impedance can be properly matched by changing the length, width, and overlapping areas of the feed strips. The resonance is made at around 866.5 MHz and -10 dB bandwidth should cover the European band of 865 MHz to 868 MHz.

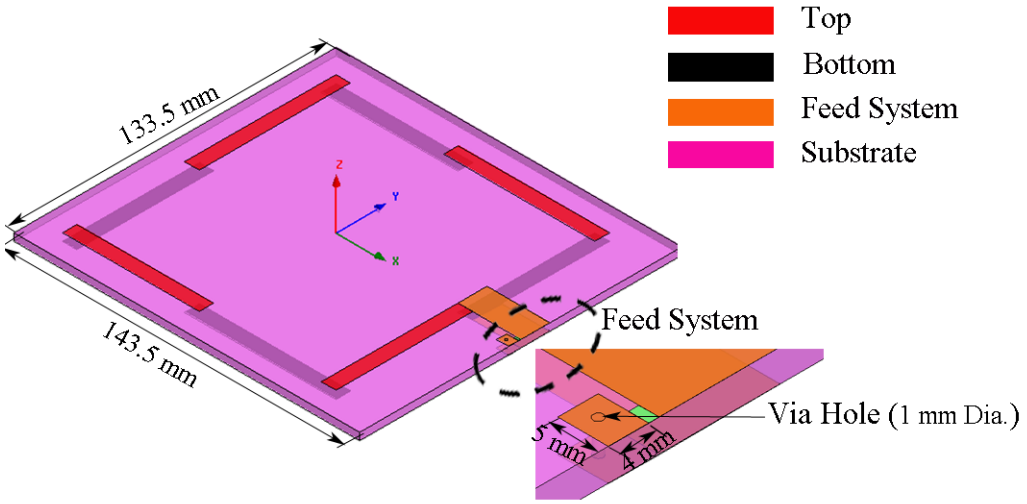

Figure 6.1: Antenna Structure for Loop Antenna.

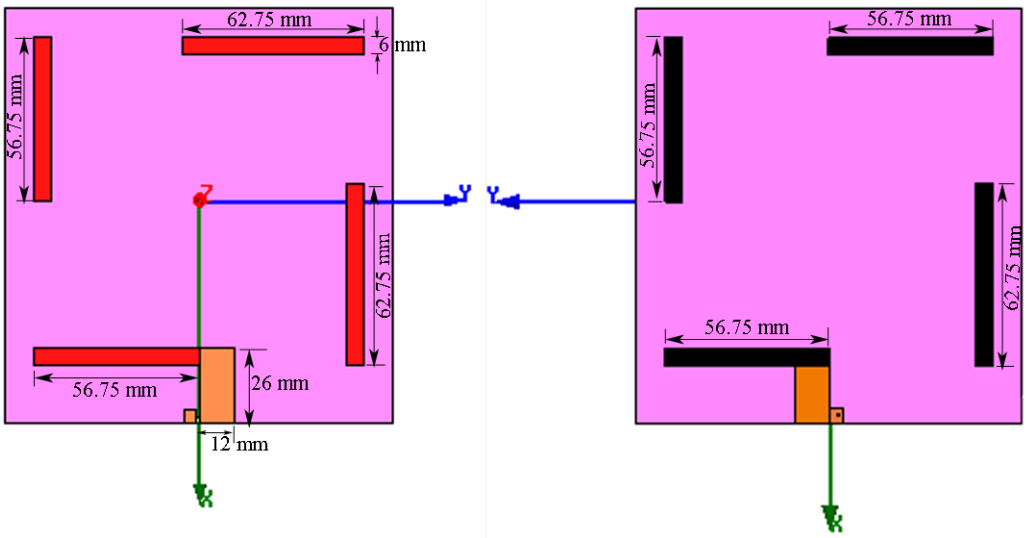

Figure 6.2: Top and Bottom View of Loop Antenna.

6.2 Simulations Results

6.2.1 S_{11} and Input Impedance

The primary task of any design is to get the proper resonance. S_{11} for the loop antenna is shown in the Figure 6.3. Considering -10 dB S_{11} as the minimal requirement, the bandwidth goes from 829 MHz to 912 MHz. This is wideband covering most of the UHF RFID band. The antenna is resonating at 866 MHz with S_{11} of -45 dB. The value of S_{11} is low enough for the desired European band.

The input impedance over 700 MHz to 1000 MHz is plotted on the Figure 6.4.

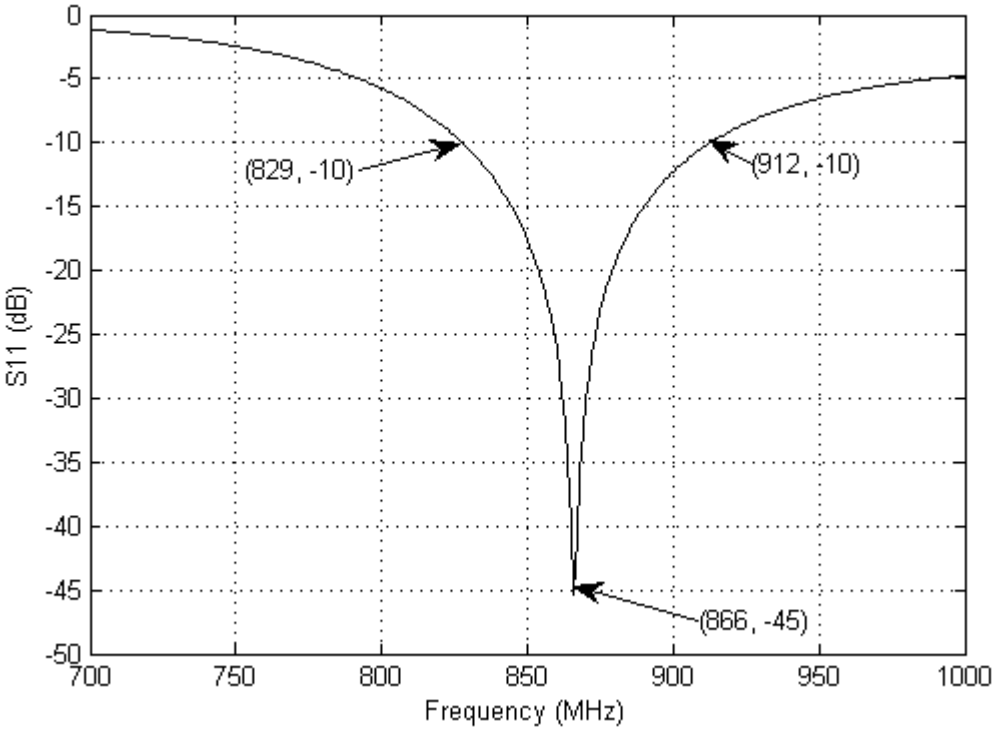

Figure 6.3: S_{11} of Loop Antenna.

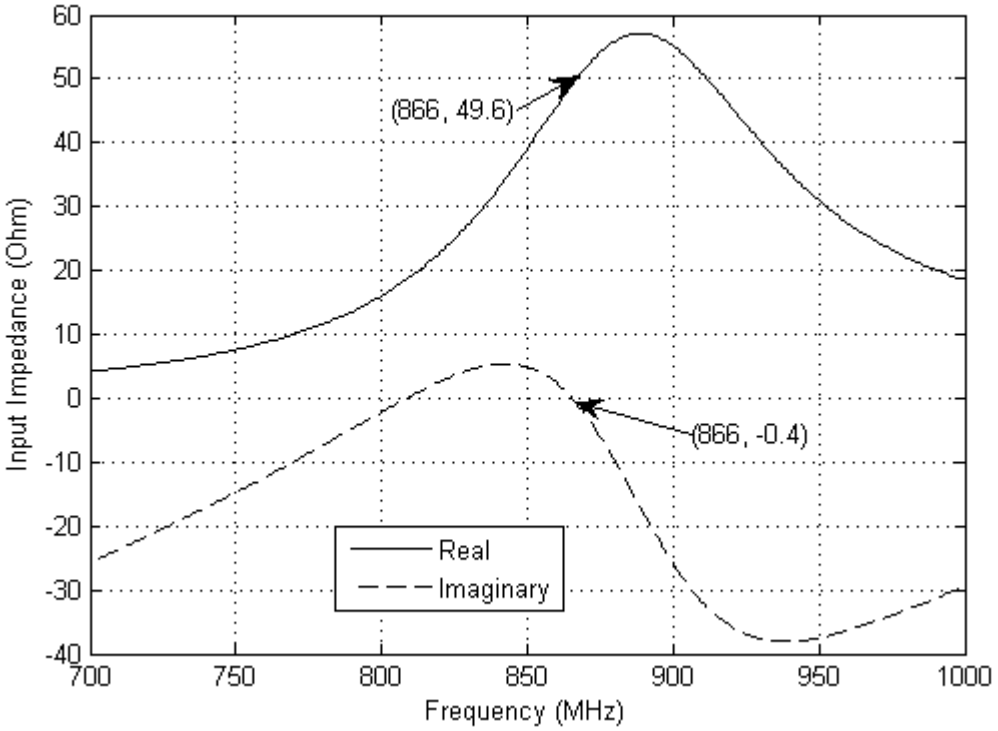

Figure 6.4: Input Impedance of Loop Antenna.

The real part is 49.6 Ω and the imaginary part is -0.4 Ω at the resonant frequency of 866 MHz. The length and the width of the feed lines have been adjusted properly to get perfect impedance matching.

6.2.2 Current and Magnetic Field Distribution

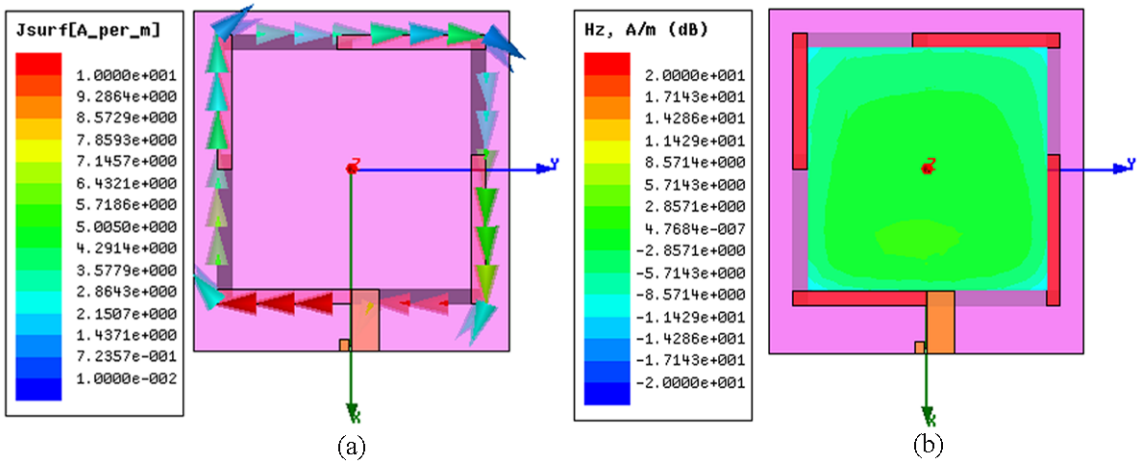

Figure 6.5: (a) Current Distribution Along Loop, and (b) Magnetic Field Distribution at $z = 20$ mm.

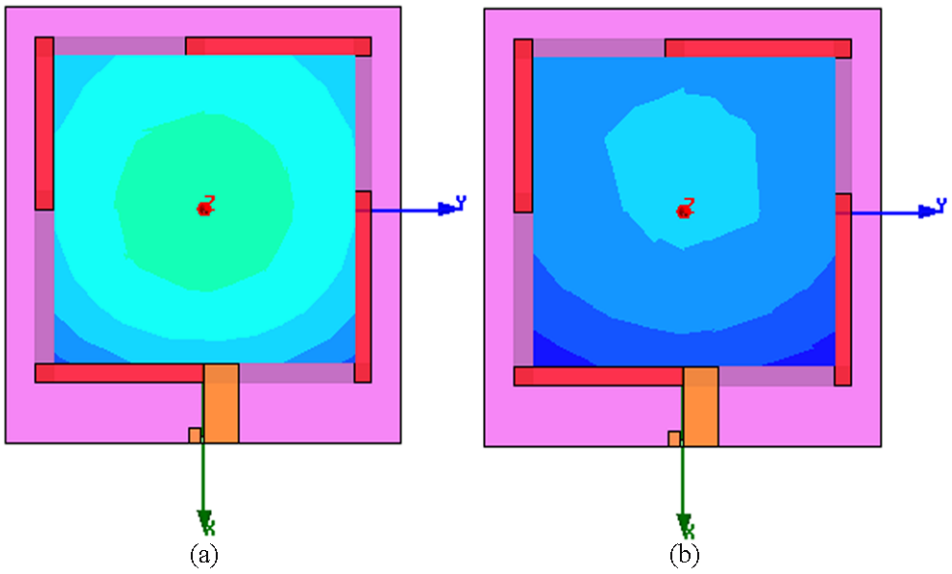

Figure 6.6: Magnetic Field Distribution at (a) $z = 60$ mm, and (b) $z = 100$ mm.

The current is flowing in the same direction and its magnitude is higher in the segments connected to the feed whereas it is almost uniform in the rest of the segments. The higher current distribution in the dipole structure radiates higher power

as compared to the other segments.

The z-component of the magnetic field should be uniform near to the antenna surface within the interrogation zone. On the otherhand, the intensity should be higher in the center region at higher distances from the antenna due to the accumulation of field resulted from all the loop segments. The fields are plotted at three different distances of 20 mm, 60 mm, and 100 mm as shown in the Figure 6.5(a), 6.6(a), and 6.6(b) respectively. The field distribution at $z = 20$ mm is uniform and those at $z = 60$ mm and $z = 100$ mm have higher values in the center region. These figures add also the information about the decay of magnetic field along $+z-$axis.

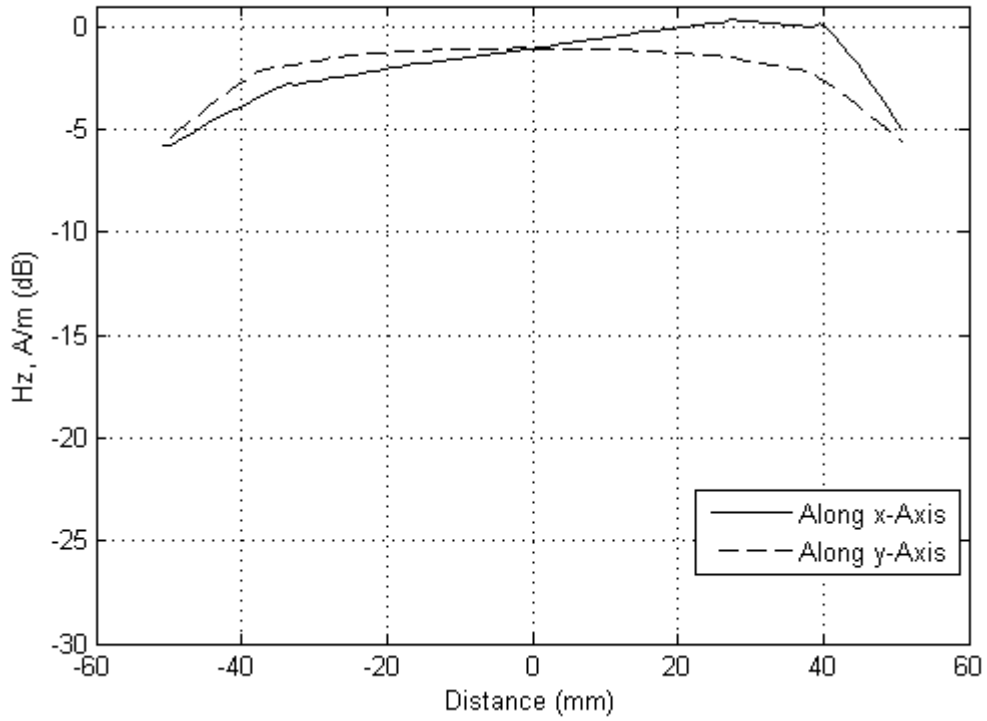

Figure 6.7: Field Distribution Along x-Axis and y-Axis.

Distribution of the magnetic field is closely studied by plotting the field along x-axis and along y-axis. It is done at $z = 20$ mm and shown in the Figure 6.7. There is a peak on the solid line near by the feed indicating the higher intensity of field due to higher current density. However, the field variation does not exceed 6 dB which implies that the field distribution is uniform in the interrogation zone.

6.2.3 Realized Gain

The expected radiation pattern is the omnidirectional along the axis (i.e., y-axis) containing the segements connected to the feed. However, the gain is more toward +x and -x-axes and less along z-axes. But, the radiation along z-axes is not too low to make the antenna unable to read the far-field tags. The radiation patterns in 3D and 2D are shown in the Figure 6.8 and 6.9

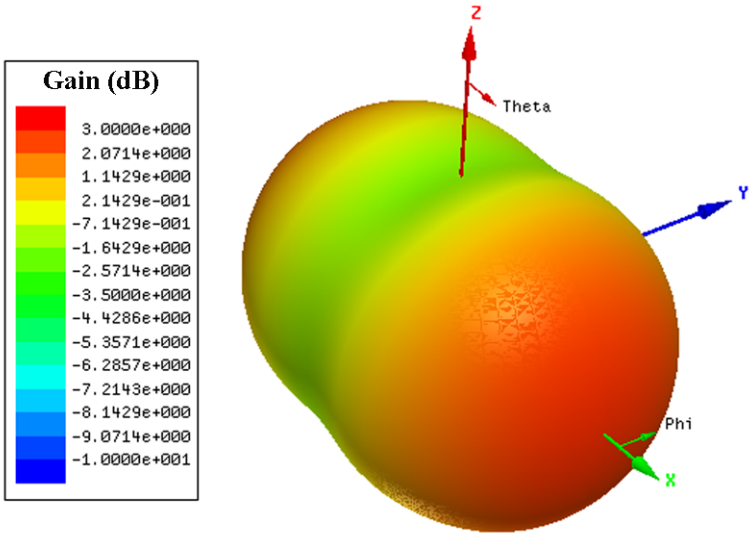

Figure 6.8: 3D Radiation Pattern of Loop Antenna.

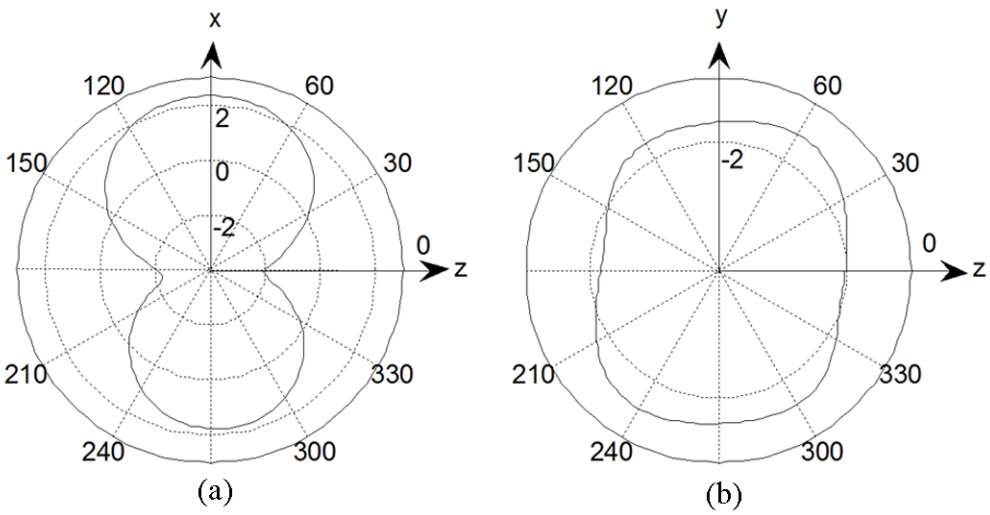

Figure 6.9: Radiation Pattern on (a) xz-plane, and (b) yz-plane.

6.3 Antenna Fabrication

The simulated loop antenna design is fabricated again by the milling process. There is high risk of displacement between top and bottom layers if not fixed properly

during milling. Rogers RT 5880 is used as the substrate. The prototype looks as given in the Figure 6.10.

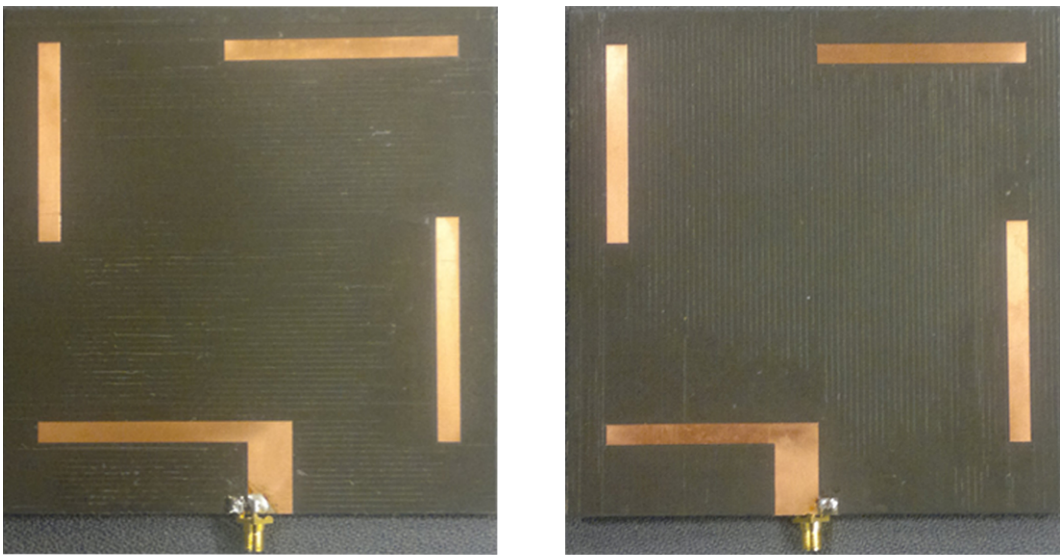

Figure 6.10: Prototype of Loop Antenna (a) Top View, and (b) Bottom View.

Regarding to the feed system, via hole is used to take the connection point from bottom layer to the top layer. And, a simple SMA connector is fitted as shown in the figure.

6.4 Measurements Results

6.4.1 S_{11} and Input Impedance

VNA is used to obtain the S_{11} and input impedance of the fabricated loop antenna. In the Figure 6.11, we can see that the measured S_{11} curve is shifted to the right by quite a large amount as compared to the simulated one. However, the -10 dB bandwidth still covers our desired band and hence it can be used in measurements and practices. The shift in resonance frequency might have different reasons. The parameters used in simulations might be different than the actual ones. There can have relative displacement between top layer and bottom layer in the milling process. The via hole modeling might not be proper. And there may be other unseen reasons behind this. However, the resonance can be easily shifted back to 866 MHz by increasing the overlapping area. Three pieces of copper tape having size around 6 mm $\times$ 6 mm have been attached to the three segments for this purpose. And, rest of the measurements except input impedance are taken with this tuned antenna.

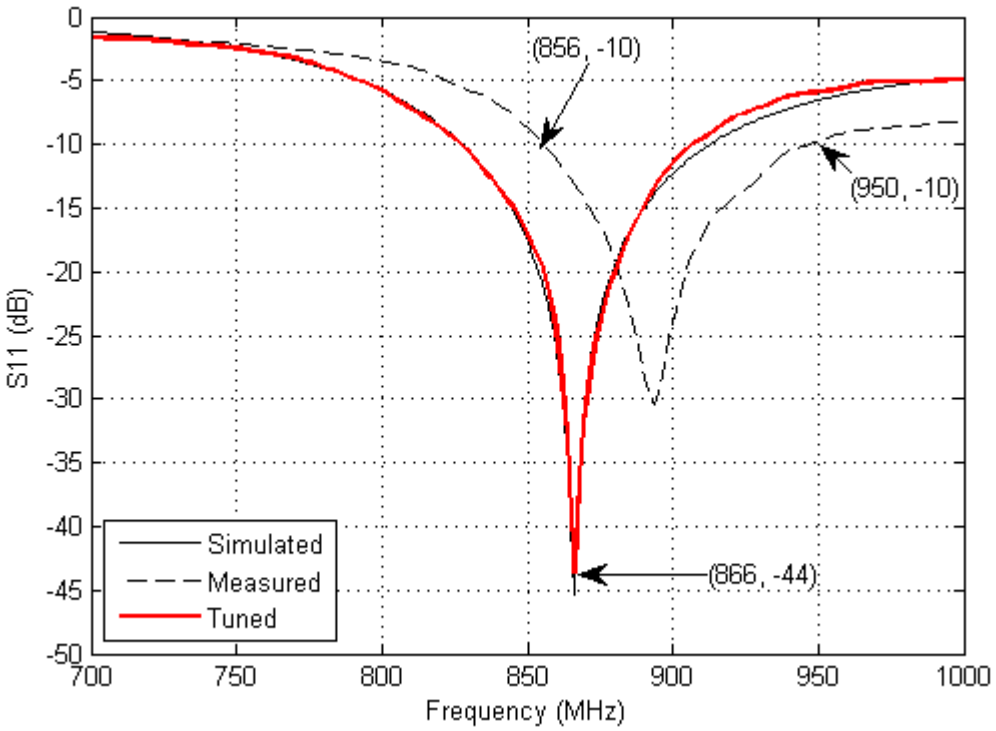

Figure 6.11: Measured S_{11} of Loop Antenna.

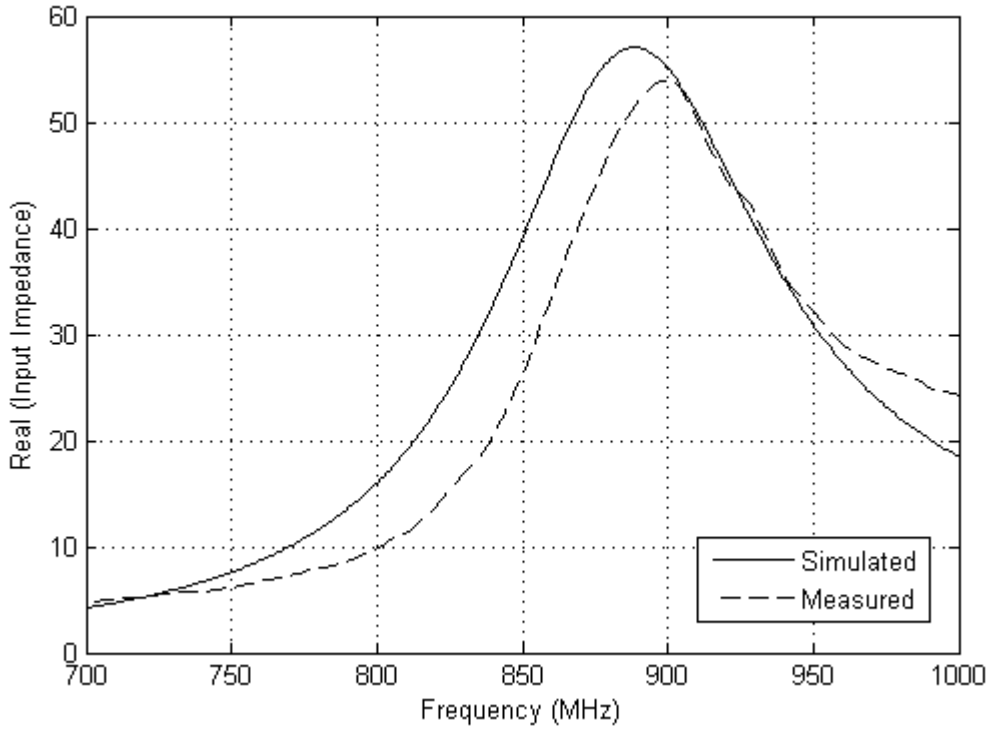

Figure 6.12: Real Part of Measured Input Impedance.

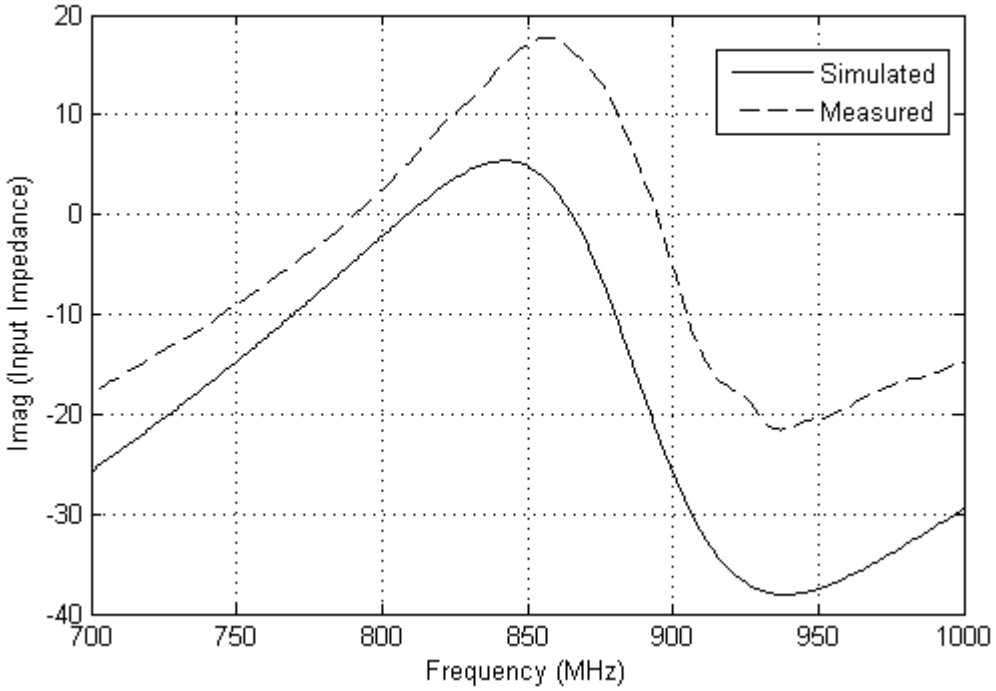

Figure 6.13: Imaginary Part of Measured Input Impedance.

The real and imaginary parts of the input impedance are plotted on the Figure 6.12 and 6.13 respectively for both the simulations and measurements. The measured curve is shifted from the simulated position thus changing the resonance frequency. The curves are not changing so rapidly being able to provide larger bandwidth.

6.4.2 Realized Gain

The radiation pattern of the fabricated antenna is measured in Satimo Starlab. The 3D view of the pattern is given in the Figure 6.14. It looks similar to the simulated pattern but the radiation toward y- and z-axes is less.

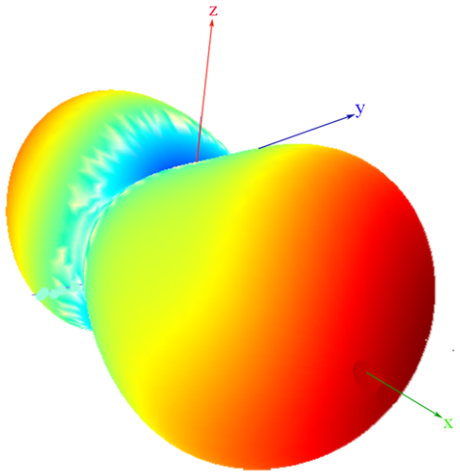

Figure 6.14: Radiation Pattern of Loop Antenna in 3D.

The radiation patterns can be plotted on the xz- and yz-planes to compare with the simulated ones. The patterns look more or less similar but the measured gain toward y- and z-axes is less than the simulated gain as shown in the Figure 6.15. However, this much of gain may be sufficient to read high gain far-field tags for couple of meters.

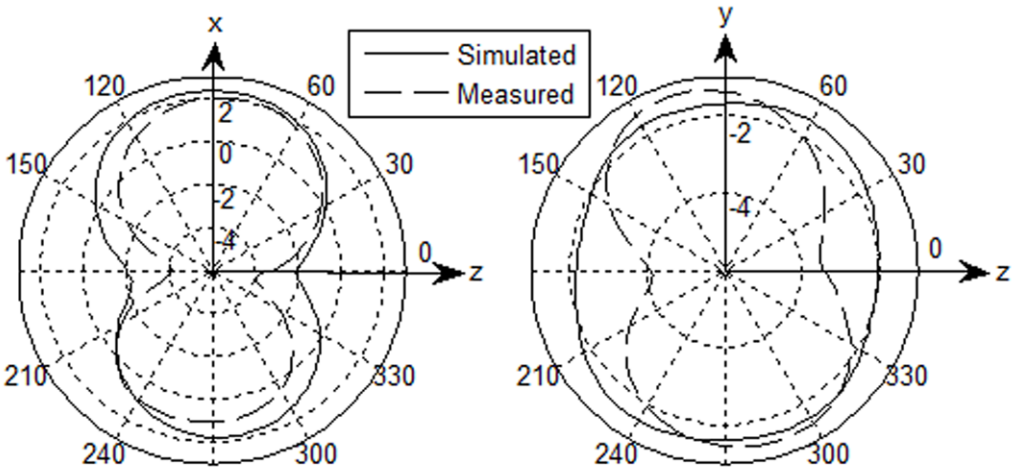

Figure 6.15: Radiation Pattern on (a) xz-Plane, and (b) yz-Plane for Loop Antenna.

6.5 Read-Range Measurements

The ultimate goal of an antenna design in RFID applications is to get good read-range in the desired direction. The primary focus in our design is the near-field read-range. Since the antenna is designed for the hand-held application and for inventory control purpose, the far-field read-range of couple of meters is sufficient. For read-range measurements, the commercial Alien RFID Reader Unit [40] is used. The measurement set up is shown in the Figure 6.16.

Figure 6.16: Measurement Set Up for Reading Performance.

6.5.1 Near-Field Measurements

The near-field button type tag of diameter 8 mm has been used for near-field read-range measurements. The measurement data are recorded from different parts of the antenna.

The read-range is higher in the center region due to higher field intensity as obtained from the simulation. The read-ranges at different positions are marked on top of the antenna as shown in the Figure 6.17. The maximum value obtained is 15 cm. However, the near-field read-range is associated with the disturbance of radiations by surrounding objects due to the impedance matching issue. Therefore, the read-range may depend on the measurement environment. The tag used for measurements is attached on the same figure right-down corner.

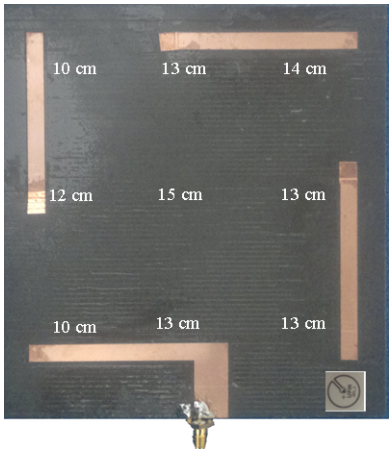

Figure 6.17: Near-Field Read-Range at Different Parts of the Loop Antenna.

The above reading performance is for tag parallel to the antenna. The read-range for tag perpendicular to the antenna is very small which is not recorded here.

6.5.2 Near-Field Measurements With Objects

In practice, tags are attached on the objects. Small sized, sensitive, and expensive objects are the main targets of near-field communication. Few samples as shown in the Figure 6.18 have been considered for measurements. The purpose of this measurement is to show the reading performance in practical scenario.

Figure 6.18: Near-Field Measurements With Objects.

The same button type tag is used here. The maximum read-range is recorded for all the objects. The maximum value is obtained when the tag on the object is located in the center region of the reader antenna. The maximum value of read-range in centimeters for all the objects are marked on their own bodies as shown in the Figure 6.18.

The read-range is not same for all the objects and is less than when measured without objects. The reason behind this can be explained in different ways. The radiation of the antenna is altered by the presence of nearby objects which can change S_{11}. This causes impedance mismatch between source and antenna. The current flowing through the loop decreases and hence the magnetic field intensity. This can decrease the near-field read-range and depending on the degree of impedance mismatch, the read-range can be different for different objects. The permeability of different objects may be different responsible for different read-ranges. By attaching the tag on the object, it is curved according to the shape of the object. This reduces the loop area of the tag and hence the magnitude of coupling. It can be explained in better way. The voltage, v induced in the tag antenna coil is [12]

$$v = -\frac{\mathrm{d}\phi}{\mathrm{d}t}, \tag{6.1}$$

and the total magnetic flux through the surface of coil is

$$\phi = \int \overrightarrow{B} \cdot \mathrm{d}\overrightarrow{S}. \tag{6.2}$$

So, the orientation and the bending of the tag which depends on the object's surface greatly affects the power absorbed by the tag and hence the read-range.

6.5.3 Far-Field Measurements

The radiation pattern of the antenna promises for the reading performance of the far-field tags, but how much? Varieties of commercial far-field tags are available in the market; mojority being the dipole type. They may have different radiation characteristics and gains and hence different read-ranges for a reference reader antenna. The read-range depends also on the sensitivity of the tag. Different tags may have different sensitivities; being the reason for different read-ranges. We have chosen some commercial far-field tags (the same used in the previous chapter) as shown in the Figure 5.20 for read-range measurements with the proposed loop antenna.

The following table provides the read-ranges for the aforementioned tags along the desired direction (+z-axis) and co-polarization. The polarization along y-axis must be stronger than along x-axis according to the current distribution of the loop. Different results are obtained for different tags. Most of the tags used in this measurement are manufactured by UPM. The product UPM SD gives the best performance with read-range about 2.5 m.

We are measuring the read-range along +z-axis, in which direction, the reader

Table 6.1: Read-Range with Different Tags.

No.	Tag	Read-Range (m)
1	UHF Reference	1.5
2	Alien 964X	2.5
3	UPM SD	2.5
4	UPM Belt	1
5	UPM DogBone	1
6	UPM Web	0.6
7	UPM Frog3D	0.6

antenna has less gain as compared to other regions. The read-range is better when the tag is moved from center region of reader antenna to ±x-direction.

6.5.4 Far-Field Measurements With Objects

UPM SD tag has been used for far-field measurements with the tag attached on different objects. The reading performance depends on the types of objects. The performance is worse with liquid and metal objects. The purpose of this measurement is not to analyze the effect of objects in the reading performance in detail, but to give the view in brief that different objects may have different read-ranges.

Figure 6.19: Read-Range for Far-Field Measurements With Objects.

The Figure 6.19 presents different objects used for the measurement and also the read-ranges marked on the corresponding objects. The read-range varies from 1.3 m to 2 m indicating different results with different objects. If we had taken the measurements with varieties of objects, we would have obtained even diverse results. The metal and liquid objects do have very small read-range with this kind of normal dipole tag.

6.6 Parametric Analysis

There are no fixed formulas while designing a loop antenna. However, it's better to know what happens when a parameter is changed. There are different parameters which should be considered in the design process. Perimeter of the loop, width of the segment, height between top and bottom layers, permittivity of the substrate, overlapping area between coupling segments, and feeding system are the important parameters for designing a loop antenna. The change in any of these parameters alters the results of the overall design. For making the design process easier, one should know where the results go when a parameter is changed in a certain way. This section deals with the parametric analysis for different parameters. It should be noted that the original design is taken as the reference and only one parameter is changed at one time. The feeding system here is kept the same. The design has perimter of 454 mm, width of 6 mm, overlapping area of 36 mm^2, substrate height of 3.175 mm, and relative permittivity of 2.2.

6.6.1 Change in Loop Size

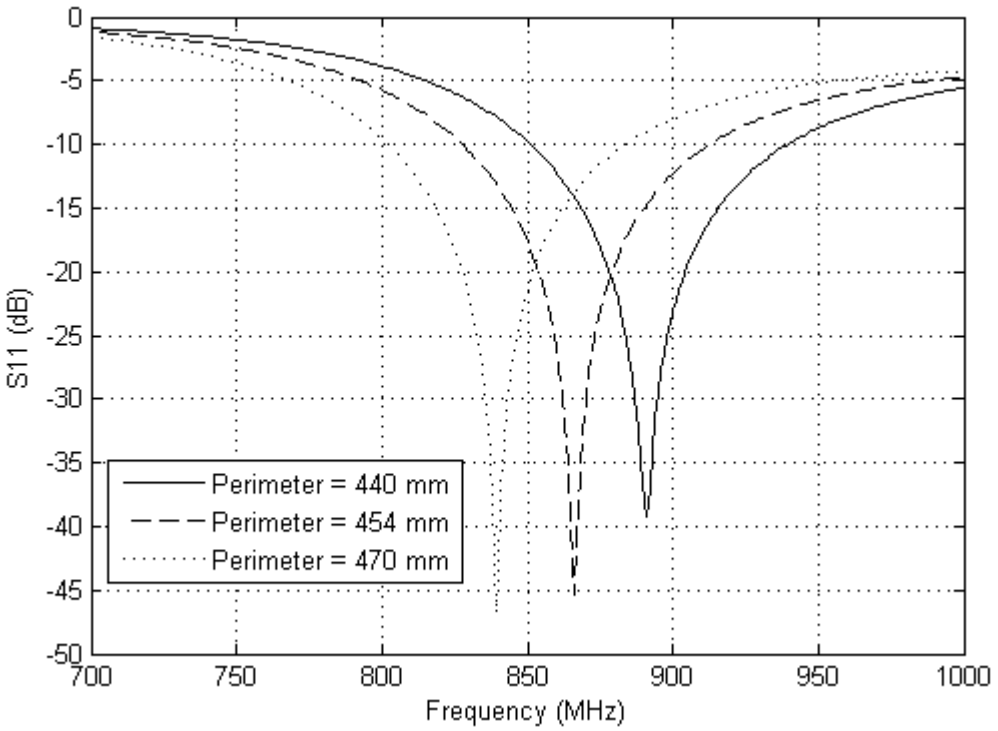

Figure 6.20: Parametric Analysis for Change in Loop Perimeter.

The major parameter in the loop antenna design is the size of the loop. The inductance depends on the length and width of the conductor. By changing the

loop size, the resonance frequency can be changed.

The results are taken for three different values of loop size: 440 mm, 454 mm, and 470 mm. All other parameters are fixed as in the original design. When the perimeter is increased, the resonance is shifted left (i.e., decreases) as shown in the Figure 6.20. For larger size, the inductance is larger. But, the overlapping area is kept constant which provides the same capacitance. According to the formula

$$f = \frac{1}{2\pi\sqrt{LC}}, \tag{6.3}$$

the resonance frequency should decrease.

6.6.2 Change in Width of Segments

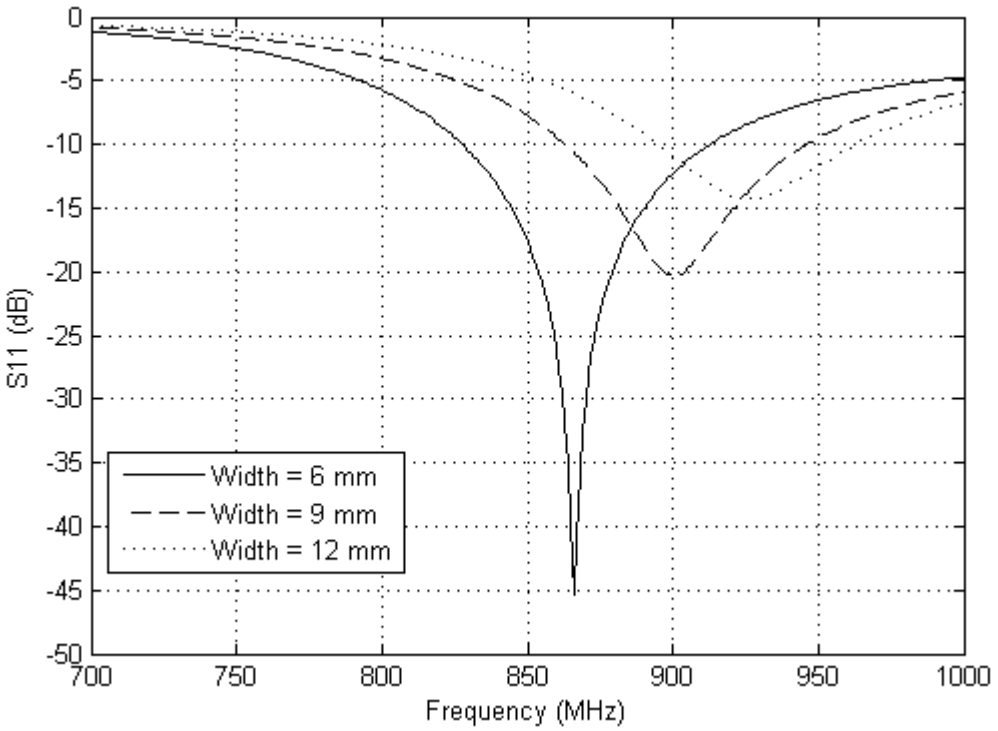

Figure 6.21: Parametric Analysis for Change in Segment Width

Perimter length here is the original size, i.e., 454 mm. We want to see how the resonance changes when width of the segments is changed. The inductance of the loop must change when its width is changed.

The Figure 6.21 shows that the resonance frequency increases when the width

is increased. So, the wider line has smaller inductance and applying the same formula (6.3), the resonance point should increase for increased width of the segments provided that the overlapping areas remain constant.

6.6.3 Change in Overlapping Areas

When two parallel plates with cross sectional area of A are separated by a dielectric of relative permittivity of ϵ_r and height of h, then the capacitance across the plates is given by

$$C = \epsilon_0 \epsilon_r \frac{A}{h}. \tag{6.4}$$

The overlapping sections of the loop segments are behaving here as the parallel plate capacitors. The capacitance produced is therefore depending on the overlapping areas between the segments, and relative permittivity and height of the substrate as illustrated by the equation (6.4).

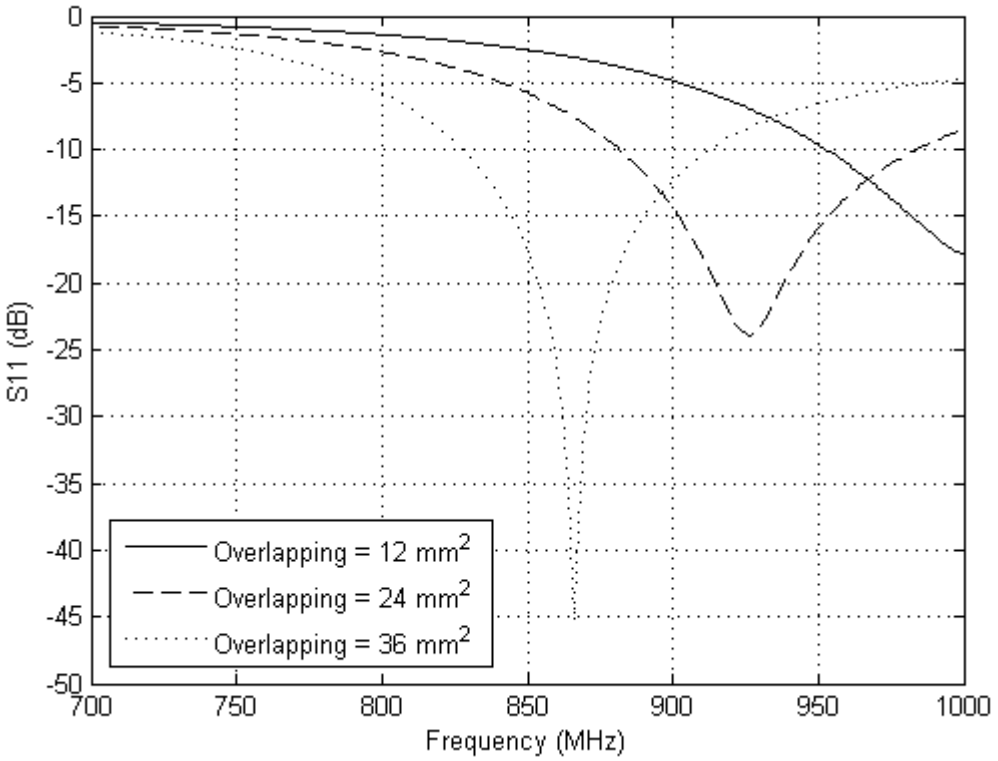

Figure 6.22: Parametric Analysis for Change in Overlapping Areas.

The loop size is again the same. Only the overlapping areas are changed. From the Figure 6.22, we can see that the resonance frequency decreases when the overlapping areas are increased. There is increase in capacitance with increase in overlapping areas which results decrease in resonance.

6.6.4 Change in Height of Substrate

It is clear from the equation 6.4 that the capacitance is inversely proportional to the height of the substrate or the separation between the plates. For higher value of h, capacitance is less and the equation 6.3 says that the resonance frequency should increase.

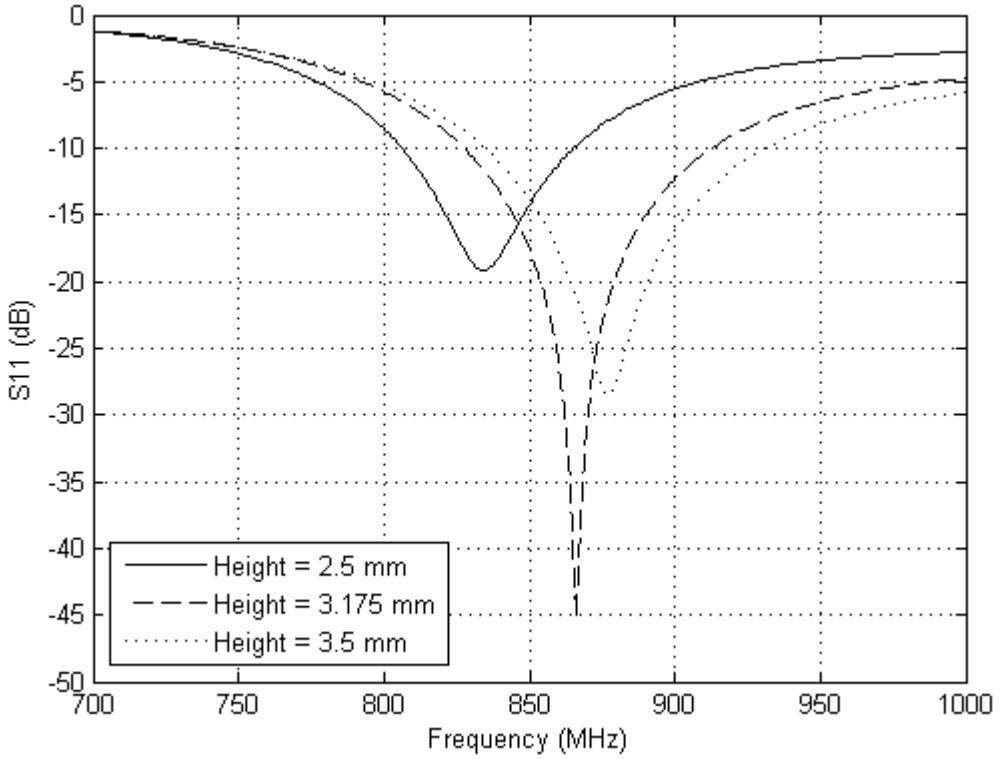

Figure 6.23: Parametric Analysis for Change in Height of Substrate.

It is true that the resonance frequency increases when the height of the substrate is increased as shown in the Figure 6.23. Only the substrate height has been changed; it's relative permittivity is still 2.2.

6.6.5 Change in Relative Permittivity

Regarding to the substrate, every parameter is similar to those of Rogerst RT 5880 substrate except the relative permittivity for this analysis. Refering to the equation 6.4 again, the capacitance is higher for higher value of relative permittivity. Since length and width of the loop segements are kept constant, the inductance is same and the increased capacitance makes the resonance frequency decrease as given by (6.3).

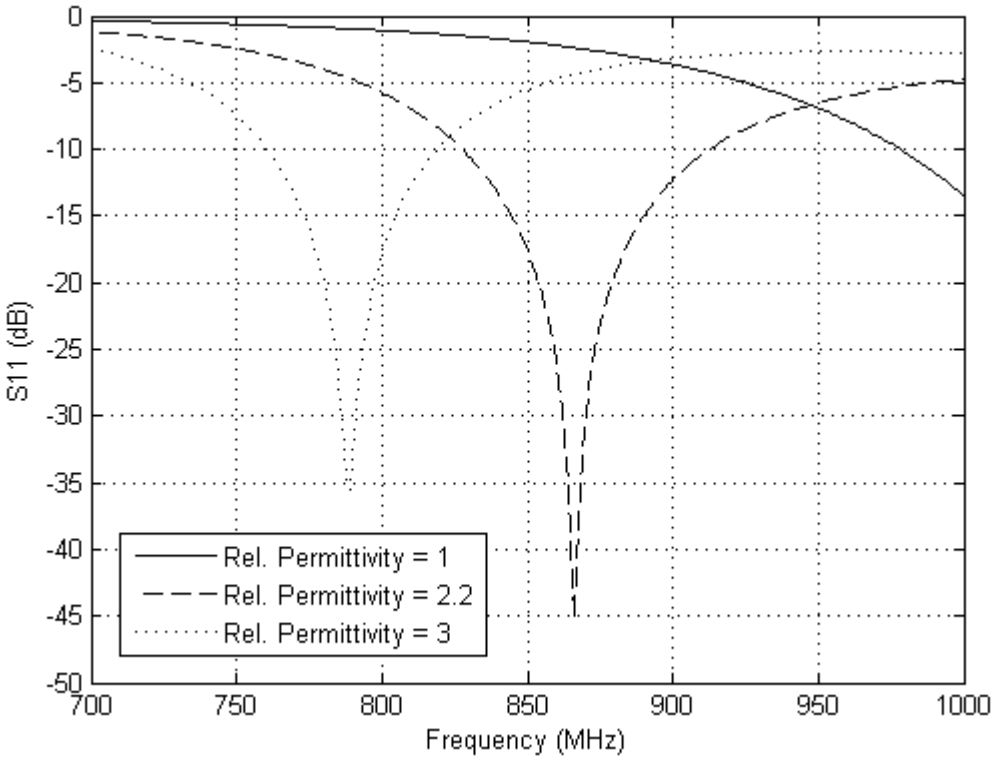

Figure 6.24: Parametric Analysis for Change in Relative Permittivity.

The Figure 6.24 supports the above explanation. The resonance frequency decreases when the relative permittivity of the substrate is increased.

7. COMPARISONS

We designed two RFID reader antennas working in European UHF band for both near field and far field. They are made to use in inventory control purpose. Incorporating two different antennas in the same structure is the challenging task. Since both the near-field and far-field antennas radiate, they interfere one another. The far-field structure can destroy the uniformity of the magnetic field of loop antenna. Impedance matching is even bigger challenging issue. The first design consists of segmented loop and patch structure whereas the second design consists of only the segmented loop. Besides near-field performance, the motif of second design is to get the proper radiation from the dipole segments connected to the source. These segments have higher current density and can act as a dipole.

The simulations and measurements were done for the first antenna. The performance was good for far-field but not satisfactory for near-field. And, some unusual results were also noticed. The patch antenna should be responsible for this. Then, the second design was made only with the loop so that we could get better near-field performance. Since the antenna is made for hand-held application, we don't need larger far-field read-range and the loop alone might give this much performance. The simulations and measurements were done for second design as well. We got better near-field performance but the far-field performance was just OK. The radiation is more toward unwanted directions.

We have commercial reader antenna [45] working in European UHF band and manufactured by Alien Technology. This is the patch antenna and is made for only the far-field application. We took measurements with this antenna also to compare the performance among all three antennas.

7.1 Simulations Comparisons

The purpose of both the designs is same. So, it's better to compare their results. We don't have any simulation result for the commercial reader antenna. Therefore, we exclude this antenna in comparisons of simulations results.

7.1.1 S_{11} Comparison

S_{11} plot gives the bandwidth of the antenna. The required band is from 865 MHz to 868 MHz, but larger than this band is not harmuful. The Figure 7.1 includes the simulated S_{11} for both the antennas.

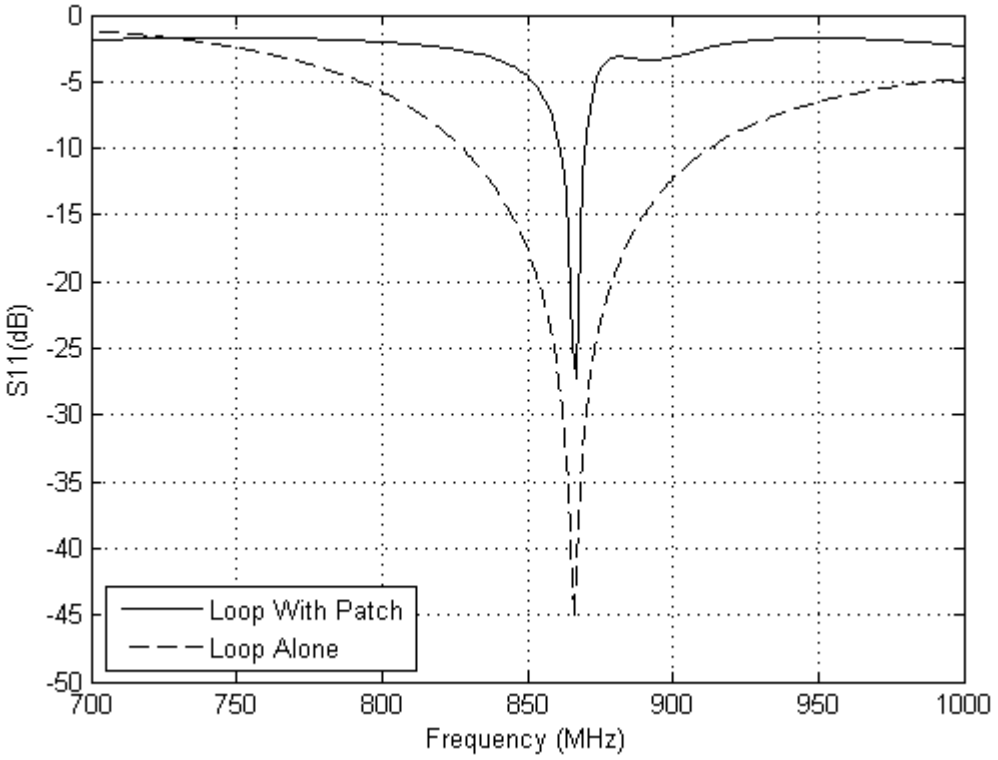

Figure 7.1: Comparison of S_{11}.

Though both the antennas are tuned at the same frequency, the second design has better S_{11} curve. The magnitude of S_{11} and the bandwidth are higher in the loop antenna without patch. Bandwidth for a patch antenna is normally low [31].

7.1.2 Current and Magnetic Field Distribution

Both the antennas have similar loop structure. The current should flow in a single direction and as uniform as possible. The z-component of the magnetic field should be uniform in the interrogation zone so that near-field tags can be detected from the entire region and the good read-range can be obtained.

From the Figure 7.2, it is noticeable that the current distribution is more uniform in the design without patch. The z-component of the magnetic field is uniformly distributed over the surface of the loop antenna, whereas it is weak at certain positions in the center part of the first design as seen clearly from the Figure 7.3.

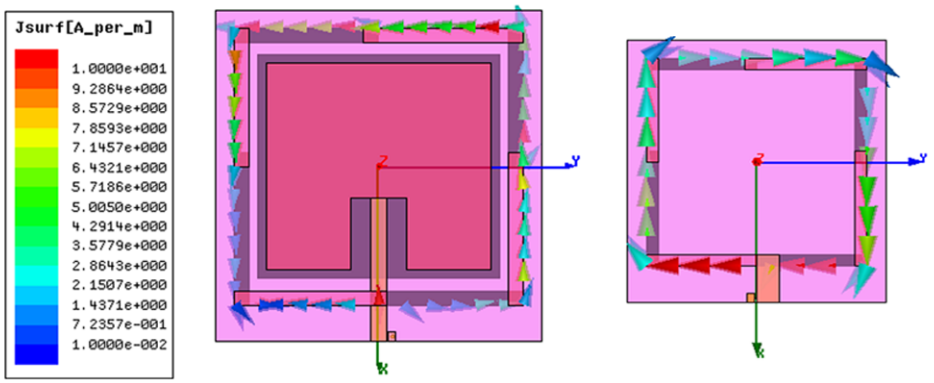

Figure 7.2: Current Distribution of the First and Second Design.

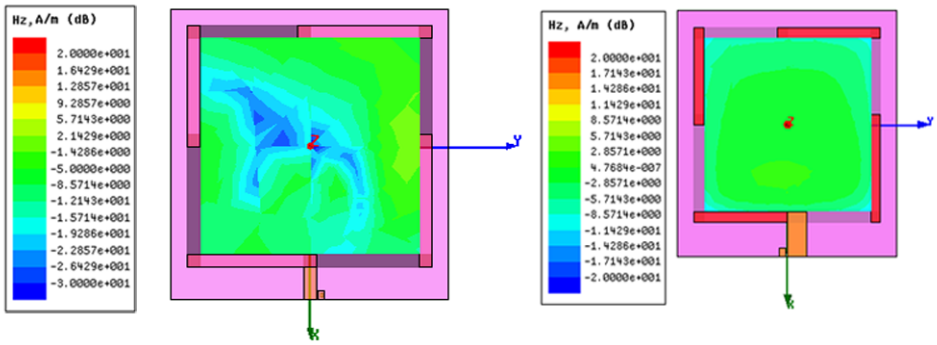

Figure 7.3: z-Component Magnetic Field Distribution of the First and Second Design at z = 20 mm.

7.1.3 Radiation Pattern

Radiation pattern is the important parameter for far-field reader antennas. It gives the idea about read-range, direction and region of detection.

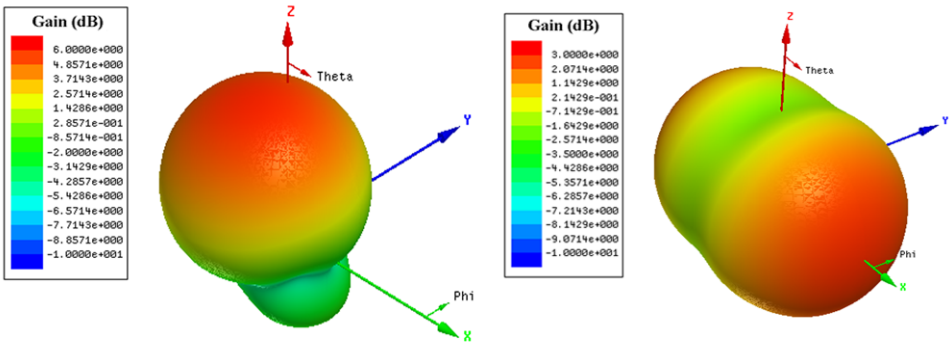

Figure 7.4: Radiation Pattern Comparison of Two Designs.

The radiation pattern is directed toward +z-axis in the first design, whereas it is directed toward ±x-axis in the second design. However, the gain along +z-axis

is good enough to read the tags for couple of meters. The Figure 7.4 clearly shows that the far-field performance should be better with the first design.

7.2 Measurements Comparisons

Prototypes are made from the simulated designs. S_{11} is measured with the help of VNA, radiation pattern in Satimo Starlab, and the reading performance with the help of Alien Reader Unit [40].

7.2.1 S_{11} Comparison

The measurements results can be different from the simulations results due to different factors. The important thing is whether the measurements results are within our specifications or not.

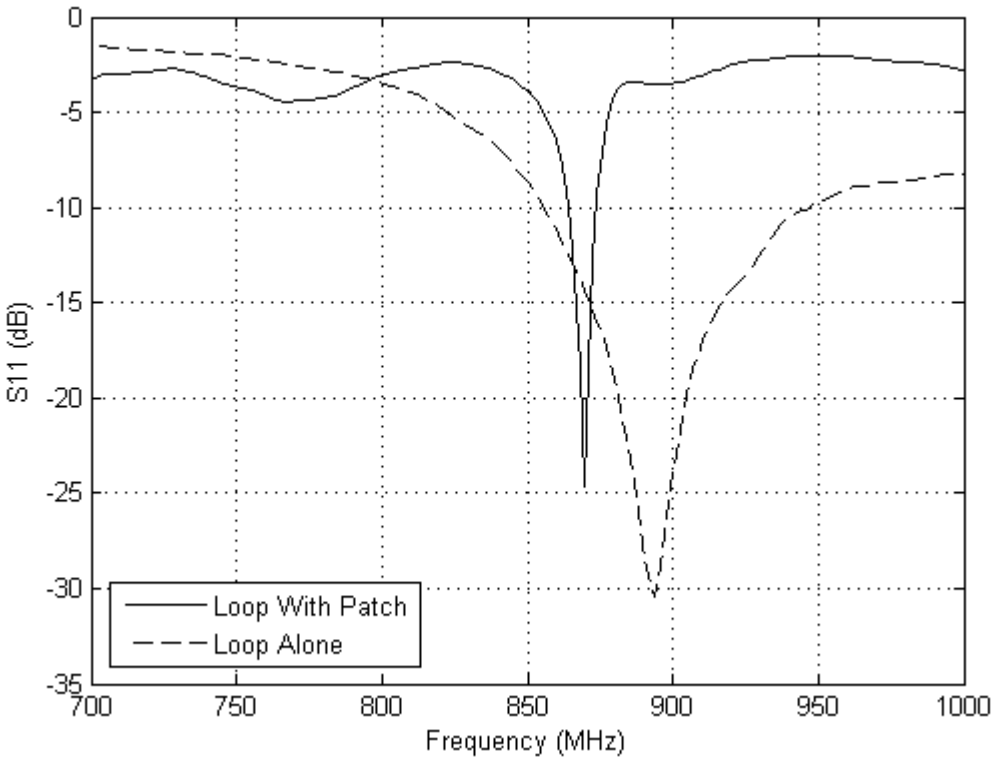

Figure 7.5: Comparison of Measured S_{11}.

The measured S_{11} for the second prototype is comparatively shifted to the right as shown in the Figure 7.5. However, the magnitude of S_{11} and the bandwidth coverage is better in the second prototype. Importantly, the bandwidth covers the whole European RFID UHF band with sufficient S_{11}.

7.2.2 Radiation Pattern Comparison

The radiation patterns of the prototypes are measured at 866.5 MHz in Satimo Starlab.

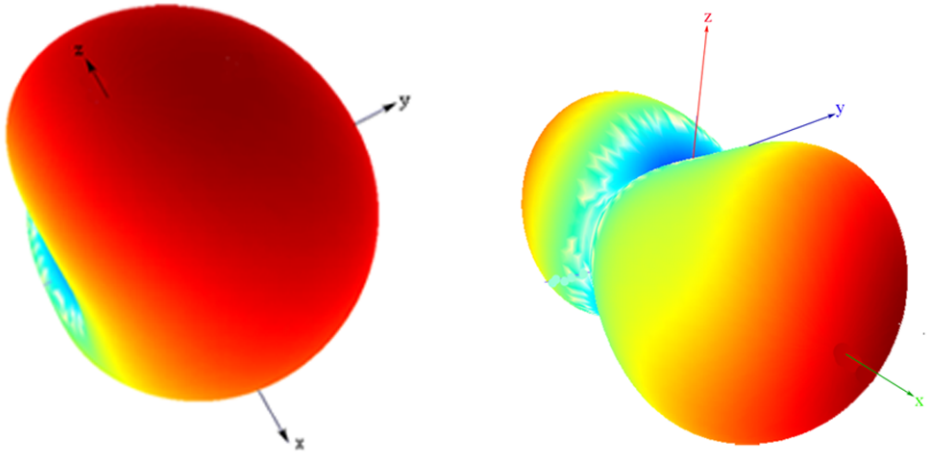

Figure 7.6: Comparison of Measured Radiation Pattern.

The radiation pattern of the first prototype is far more better than the second prototype as shown in the Figure 7.6. The radiation of the second prototype toward +z-axis is pretty weak.

7.2.3 Comparison of Near-Field Measurements

The simulations results show that the second protoype should have better near-field performance. For comparison, near-field measurement is taken also for the commercial reader antenna.

When the near-field button type tag is parallel to the antenna, the commercial antenna has negligibly small read-range. Whereas our antennas have good performance. The read-range is more stable and higher for the second prototype, whereas the read-range varies a lot and better in the region near to the loop for the first prototype.

There is one unusual near-field performance by the first prototype. When the tag is perpendicular to the antenna and on xz-plane, the antenna has more stable reading performance for 5 cm and again starts from 11 cm away for couple of centimeters. But, the performance is poor when tag is placed on yz-plane. The commercial antenna was used for the measurements in the same scenario. The results were pretty much similar. It confirms that the unusual behaviour of the first prototype is due to the patch structure. The similar measurements with the second prototype give

poor performance. The reading performance in these scenarios are unwanted.

7.2.4 Comparison of Far-Field Measurements

The simulations results for far-field operation emphasize that the first prototype should have superior far-field performance. Since the gain of the second prototype in +z-axis is not negligibly small, we can expect something for far-field.

Different far-field tags as given in the Figure 5.20 are used to measure the read-range of commercial antenna and our antennas in the desired direction for comparison. The following table gives the comparison overview of read-range for the reader antennas with different tags.

Table 7.1: Far-Field Read-Range Comparison of Reader Antennas.

No.	Tag	Read-Range (m)		
		Commercial	Prototype 1	Prototype 2
1	UHF Reference	>5	>5	1.5
2	Alien 964X	>5	>5	2.5
3	UPM SD	>5	>5	2.5
4	UPM Belt	4	3.5	1
5	UPM DogBone	2.5	2	1
6	UPM Web	2.5	2	0.6
7	UPM Frog3D	2.5	2	0.6

8. CONCLUSION

RFID technology is the blooming industry for wireless auto-identification applications. Its popularity goes on increasing with continual reduction of tag's size and price. It's been used in supply chain management system where tracking of objects begins from production level to the point of sale. The inventory control is needed to keep the objects in track in supply chain management. Reader antennas and reader units are placed at different places to keep and update the information about the products. The promising performance of segmented loop antenna at UHF band for item level tracking of small, sensitive, and expensive products leads to the research interest in this field. Not only the near-field operation but also the far-field performance may be required in the inventory control depending on the objects and applications. The objective of this thesis is to design reader antennas that can read both the near-field and far-field tags at European UHF band.

At UHF band, the required size of the loop for near-field antenna is electrically large. The current distribution is not uniform in this case which results the non-uniform magnetic field in the near-field. The motif of designing a near-field reader antenna is to make the loop size electrically small. This can be done by segmenting the loop and inserting the capacitors in between the segments. The segmented loop is the basic requirement for uniform near-field operation at UHF. Though the loop itelf has radiation characteristic, it may be along the unwanted direction. There needs to be implemented a far-field structure as well to make the antenna work for both the fields. Normally, dipole and patch structures can be used for far-field operation.

This thesis report presents two reader antennas for near-field and far-field at European UHF band. The first design consists of segmented loop and patch. Near-field reading is performed by loop antenna, whereas far-field reading is carried by patch antenna. Loop is segmented into eight parts and the segments are arranged on top and bottom of the substrate alternatively so that there is certain overlapping region between the consecutive top and bottom layers to produce capacitive effect. The operating frequency chosen is 866.5 MHz. Rogers RT 5880 is used as the substrate which has relative permittivity of 2.2 and height of 3.175 mm. Rectangular patch

antenna with inset type microstrip feed is used inside the loop. For larger bandwidth and efficiency, the substrate thickness should be larger and permittivity should be smaller. Moreover, the ground plane should be large enough to prevent back lobe radiation significantly. Despite of different compromises, the first antenna is designed in HFSS software and prototype is made for measurements.

The simulated antenna has bandwidth from 861 MHz to 870 MHz. Milling machine is used to fabricate the antenna. The fabricated antenna has bandwidth from 864 MHz to 873 MHz which is good enough for European UHF band. Near-field and far-field read-range is measured with the help of Alien Reader for different commercial tags. UPM button type tag of 8 mm diameter is used as the reference tag for near-field performance and UPM SD tag for far-field performance. With these tags, the near-field read-range can go up to 9 cm, whereas the far-field read-range is greater than 5 m. The radiation pattern is measured in Satimo Starlab which is almost similar to the simulated pattern. Radiation is along +z-direction as the requirement. Far-field reading performance is satisfactory and near-field reading is good in the peripheral regions but weak in the center region. For small part in the center, the antenna cannot detect the near-field tag. This must be due to the presence of patch antenna. Larger far-field read-range is generally not required for hand-held devices. Therefore, the second design is made for better near-field performance and quite OK far-field read-range.

The second design consists of the segmented loop as in the first design but there is no patch antenna embedded in the new design. The idea here is to make the two segments connected to the feed as the dipole structure which has higher current density as compared to the other segments. Then, this dipole structure can be used for far-field operation. The loop size, width, and overlapping area are different from the first antenna for tuning the antenna to the right frequency in the absence of patch structure. The substrate material is again the Rogers RT 5880.

The simulated bandwidth is from 829 MHz to 912 MHz which is wideband as compared to that of the first antenna. Prototype is made for the second design as well by milling process. The fabricated antenna is measured for S_{11} with the help of VNA. The bandwidth obtained is from 856 MHz to 950 MHz which is shifted to the right as compared to the simulated one. However, this covers the whole desired band with good magnitude of S_{11}. Small pieces of copper tape can be added to some segments to shift the resonance back to the right place. Different commercial tags are used to measure the near-field and far-field read-ranges. UPM button type tag and UPM SD tag are used as the references for near-field and far-field performances

respectively. The maximum near-field read-range is 15 cm from the center part and the far-field read-range is 2.5 m when measured with reference tags. The radiation pattern is measured in Satimo StarLab.

The first antenna has good far-field performance and poor near-field performance. On the other hand, the second antenna has good near-field performance and just OK far-field performance. It is clear to see that there is compromise between far-field and near-field performances in these two designs. The central part of the first antenna has poor near-field performance, whereas it is better for the second antenna. The radiation pattern of the first antenna is along +z-axis, whereas that of the second antenna is along x-axis. Though the radiation toward +z-axis is weak, the second antenna can read UPM SD 273_1 far-field tag up to 2.5 m which is sufficient for hand-held applications.

Thus, these two antennas can be used for inventory control purpose at European UHF band where both the near-field and far-field operations are required. However, it is better to modify these designs so that the near-field peformance is uniform from the entire area of the antenna and the radiation pattern is along only the desired direction. The radiation can be directed toward the desired direction by using the reflector in the required place. Instead of the big normal patch antenna, we can use the miniaturized patch antenna to reduce its effect in the near-field performance. In the second design, some modifications in the dipole like structure may give the better radiation pattern.

BIBLIOGRAPHY

[1] D. M. Pozar, *Microwave Engineering*. John Wiley and Sons, 2005.

[2] Reitz, Milford, and Christy, *Foundations of Electromagnetic Theory*, Fourth Edition. Addison Wesley Longman, 1993.

[3] W. H. Hayt, and J. A. Buck, *Engineering Electromagnetics*, Seventh Edition. New Delhi: McGraw-Hill, 2008.

[4] R. Want, "An introduction to RFID technology," *IEEE Pervasive Comput.*,vol. 5, no. 1, pp. 25-33, Jan.-March 2006.

[5] P. Adamcova, and Z. Tobes, "UHF RFID Technology and its Applications," *IEEE 17th International Conference, Radioelektronika*, April 2007, pp. 1-5.

[6] D. M. Dobkin, *The RF in RFID*. UK: Elsevier, 2008.

[7] K. Finkenzeller, *RFID Handbook*, Second Edition. England: Wiley, 2003.

[8] R. Weinstein, "RFID: a technical overview and its application to the enterprise," *IEEE Journals on IT Professional*, vol. 7, no. 3, pp. 22-33, August 2005.

[9] Rules and Regulations, Federal Communications Commission (FCC), Part 15.247: Radio Frequency Devices, March 2010. Available: www.fcc.gov

[10] Regulatory Status for using RFID in the UHF Spectrum, EPCglobal, December 2010. Available: www.gs1.org/docs/epcglobal/UHF_Regulations.pdf

[11] European Telecommunications Standards Institute (ETSI). Available: www.etsi.org, 2010

[12] S. Chen, and V. Thomas, "Optimization of inductive RFID technology," *IEEE International Symposium on Electronics and the Environment*, May 2001, pp. 82-87.

[13] X. Qing and Z. N. Chen, "UHF near-field RFID antennas," *International Workshop on Antenna Technology (iWAT)*, March 2010, pp. 1-4.

[14] P. V. Nikitin, K. V. S. Rao, and S. Lazar, "An Overview of Near Field UHF RFID," *IEEE International Conference on RFID*, March 2007, pp. 167-174.

[15] T. Lecklider, "The world of the near field," Evaluation Engineering, October 2005. Available: http://www.evaluationengineering.com/index.php/solutions/emcesd/emergency-department-helps-nj-hospitals-achieve-top-ranking.html

[16] X. Qing, C. K. Goh, and Z. N. Chen, "UHF near-field RFID reader antenna," *IEEE Microwave Conference*, December 2009, pp. 2383-2386.

[17] X. Li, J. Liao, Y. Yuan, and D. Yu, "Segmented Coupling Eye-Shape UHF band near-field antenna design," *IEEE Microwave Conference*, Dec. 2009, pp. 2401-2404.

[18] X. Qing, Z. N. Chen, and A. Cai, "Multi-loop antenna for high frequency RFID smart shelf application,"*IEEE Antennas and Propagation Society International Symposium*, June 2007, pp. 5467-5470.

[19] R. Bansal, "Near-field magnetic communication," *IEEE Antennas and Propagation Magazine*, vol. 46, no. 2, pp. 114-115, April 2004.

[20] D. M. Dobkin and S. M. Weigand, "Environmental effects on RFID tag antennas," *IEEE International Microwave Symposium Digest*, June 2005.

[21] X. Qing, Z. N. Chen, and C. K. Goh, "Platform effect on RFID tag antennas and co-design considerations," *IEEE Microwave Conference*, Dec. 2008, pp. 1-4.

[22] D. Desmons, "UHF Gen 2 for item-level tagging," presented at RFID World 2006. Available: http://www.impinj.com/files/Impinj_ILT_RFID_WORLD.pdf

[23] C. Ajluni, "Item-level RFID takes off," RF Design magazine, Sept. 2006.

[24] X. Qing, C. K. Goh, and Z. N. Chen "A Broadband Near-Field UHF RFID Antenna," *IEEE Transactions on Antennas and Propagation*, vol. 58, no. 12, pp. 3829-3838, Dec. 2010.

[25] A. L. Popov, O. G. Vendik, and N. A. Zubova, "Magnetic Field Intensity in Near Field Zone of Loop Antenna for RFID Systems," *Technical Physics Letters*, vol. 36, no. 10, pp. 882-884, 2010.

[26] D. M. Dobkin, S. M. Weigand, and N. Iye, "Segmented Magnetic Antennas for Near-field UHF RFID," *Microwave Journal*, vol. 50, no. 6, 2007.

[27] D. W. Liu, K. H. Wu, and C. F. Yang, "UHF reader loop antenna for near-field RFID applications," *Electronics Letters*, vol. 46, no. 1, Jan. 2010.

[28] X. Qing, C. K. Goh, and Z. N. Chen, "Segmented loop antenna for UHF near-field RFID applications," *Electronics Letters*, vol. 45, no. 17, pp. 872-873, August 2009.

[29] R. Hasse, V. Demir, W. Hunsicker, D. Kajfez, and A. Elsherbeni, "Design and Analysis of Partitioned Square Loop Antennas," *Journal of the Applied Computational Electromagnetics Society (ACES)*, vol. 23, no. 1, pp. 53 - 61, March 2008.

[30] Z. Frank, "Low profile near field antenna for RFID application," *IEEE International Conference on Microwaves, Communications, Antennas and Electronic Systems*, May 2008.

[31] C. A. Balanis, *Antenna Theory, Analysis and Design*, Third Edition. New York: Wiley, 2005.

[32] J. D. Kraus, *Antennas*, Second Edition. McGraw-Hill, 1988.

[33] R. A. Oliver, "Broken-loop RFID reader antenna for near field and far field UHF RFID tags," United States Design Patent D570, 337 S, Jun. 3, 2008.

[34] X. Qing and Z. N. Chen, "Antenna For Near Field And Far Field Radio Frequency Identification," United States Patent Application Publication US 20100026439 A1, Feb.4 2010.

[35] Pei-Ju Lin, Hsien-Chiao Teng, and Yu-Jung Huang, "Design of patch antenna for RFID reader applications," *IEEE 3rd International Conference on Anti-Counterfeiting, Security, and Identification in Communication*, August 2009, pp. 193-196.

[36] Wen-Shan Chen, and Yu-Che Huang, "A Novel RFID Reader Antenna with Circular Polarizatin Operation," *IEEE International Conference on Applications of Electromagnetism and Student Innovation Competition Awards (AEM2C)*, August 2010, pp. 117-120.

[37] Z. N. Chen, X. Qing, and H. L. Chung, "A Universal UHF RFID Reader Antenna," *IEEE Transactions on Microwave Theory and Techniques*, vol. 57, no. 2, pp. 1275-1282, May 2009.

[38] P. V. Nikitin and K. V. S. Rao, "Helical antenna for handheld UHF RFID reader," *IEEE International Conference on RFID*, April 2010, pp. 166-173.

[39] Ansoft HFSS Software. Available: http://www.ansoft.com/products/hf/hfss.

[40] RFID Reader Unit. Available: http://www.alientechnology.com/docs/ALR-8780_HR_DSA4F.pdf.

[41] UHF Reference Tag. Available: http://www.voyantic.com/assets/TFl.pdf.

[42] Alien Tag 964X. Available:
http://www.alientechnology.com/tags/index.php.

[43] UPM Tags. Available:
http://www.upmrfid.com/rfid/rfid.nsf/sp3?open&cid=uhf-rfid-products.

[44] P. Raumonen, L. Sydanheimo, L. Ukkonen, M. Keskilammi, and M. Kivikoski, "Folded dipole antenna near metal plate," *IEEE Antennas and Propagation Society International Symposium*, vol. 1, pp. 848-851, June 2003.

[45] Alien RFID Reader Antenna Datasheet. Available:
http://www.prosign.dk/en/rfid-products/rfid-antenner.